in the detection of an HIV-1 load >50 copies/mL in some of the patients whose HIV-1 load had been undetectable (<50 copies/mL) by the Amplicor Monitor over several years and for whom antiretroviral treatment regimens had not been changed [1, 2].

A total of 1387 HIV-1–infected patients visited our outpatient clinic from March through June 2008, and their HIV-1 load was measured by the TaqMan assay. Among these patients, 876 regularly visited the clinic (once every 1–3 months) and had an undetectable HIV-1 load by the Amplicor Monitor at the last visit. Surprisingly, the TaqMan assay detected an HIV-1 load >50 copies/mL in 253 (28.9%) of the 876 patients, although antiretroviral treatment had not been modified for these patients. Furthermore, another 22 patients (2.5%) were found to have an HIV-1 load >40 copies/mL with use of the TaqMan assay. The same assay also detected HIV-1 RNA at levels lower than the linear range of the assay (<40 copies/mL) in 128 (14.6%) of the 876 patients.

We analyzed the relationship between TaqMan detectability and time during which the HIV-1 load was undetectable by the Amplicor Monitor. This time was defined as the period from the first HIV-1 load undetectable by the Amplicor Monitor to the viral load first measured by the TaqMan assay, without any HIV-1 load rebound or blip detected during the period. Interestingly, among the patients who had a viral load undetectable by the Amplicor Monitor for <1 year, 43.7% had an HIV-1 load >50 copies/mL detected by the TaqMan assay; among the patients who had a viral load undetectable by the Amplicor Monitor for >4 years, 18.5% had an HIV-1 load >50 copies/mL detected by the TaqMan assay (figure 1). Conversely, 37.3% of patients who had a viral load undetectable by the Amplicor Monitor for <1 year had HIV-1 RNA undetectable by the TaqMan assay, and 70.2% of patients who had a viral load undetectable by Amplicor Monitor for >4 years had an HIV-1 load undetectable by the TaqMan assay. Thus, the proportion of patients who had an HIV-1 load >50 copies/mL was inversely correlated with the duration that the viral load was undetectable ($R^2 = 0.895$), and the proportion of patients with undetectable viral load was positively correlated with the duration that the viral load was undetectable ($R^2 = 0.979$). These findings indicate that the longer the effective treatment, the greater the number of patients with HIV-1 RNA undetectable by the TaqMan assay.

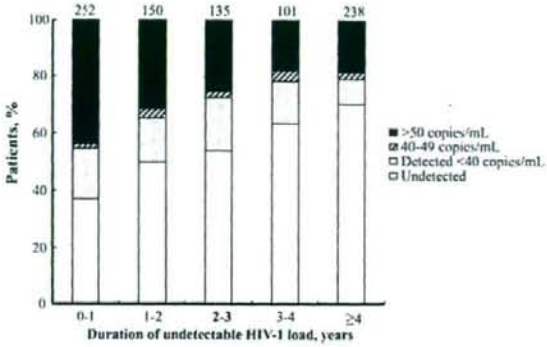

Figure 1. Results of the TaqMan assay and duration of undetectable HIV-1 load in 876 patients whose HIV-1 load was undetectable (<50 copies/mL) when the last Amplicor Monitor was performed. The number of patients is shown above each bar.

We observed significant discrepancy of HIV-1 detectability between the TaqMan assay and the Amplicor Monitor [3–5]. The TaqMan assay detected HIV-1 RNA in a significant percentage of treated patients with HIV-1 loads previously undetectable by the Amplicor Monitor; this is confusing to clinicians and patients and may be a critical problem in ongoing clinical trials of antiretroviral treatment. To determine the permissible range of detectable HIV-1 load during successful antiretroviral treatment, year-long clinical follow-up of treated patients is necessary. Our observation revealed that the detection rate of HIV-1 RNA with use of the TaqMan assay was inversely correlated with the previous duration of undetectable HIV-1 load, suggesting that long-term antiretroviral treatment can further suppress HIV-1 load even after it has decreased to below the detection limit of the Amplicor Monitor.

Acknowledgments

We thank Drs. Mahoko Kamimura, Kouji Watanabe, and Kunio Yanagisawa, for their helpful discussion and continuous support, and the nurses of AIDS Clinical Center Outpatient Clinic and the AIDS Clnical Center coordinator nurses, for their dedicated assistance.

Financial support. Ministry of Health, Labor, and Welfare of Japan grant-in-aid for AIDS research (H20-AIDS-002).

Potential conflicts of interest. All authors: no conflicts.

Hiroyuki Gatanaga, Kunihisa Tsukada, Haruhito Honda, Junko Tanuma, Hirohisa Yazaki, Tamayo Watanabe, Miwako Honda, Katsuji Teruya, Yoshimi Kikuchi, and Shinichi Oka

AIDS Clinical Center, International Medical Center of Japan, Tokyo, Japan

References

1. Erali M, Hillyard DR. Evaluation of the ultrasensitive Roche Amplicor HIV-1 Monitor assay for quantitation of human immunodeficiency virus type 1 RNA. J Clin Microbiol **1999**; 37: 792–5.
2. Perrin L, Pawlotsky JM, Bouvier-Alias M, Sarrazin C, Zeuzem S, Colucci G. Multicenter performance evaluation of a new TaqMan PCR assay for monitoring human immunodeficiency virus RNA load. J Clin Microbiol **2006**; 44:4371–5.

High frequency and proliferation of $CD4^+FOXP3^+$ Treg in HIV-1-infected patients with low CD4 counts

Xiuqiong Bi[1], Yasuhiro Suzuki[2], Hiroyuki Gatanaga[1] and Shinichi Oka[1]

[1] AIDS Clinical Center, International Medical Center of Japan, Tokyo, Japan
[2] Department of Infectious and Respiratory Diseases, Tohoku University, Miyagi, Japan

The frequency of Treg is reported to be higher in patients with chronic HIV type 1 (HIV-1) infection and $CD45RA^+$ Treg exist in normal adults. In this study, we found a lower absolute number (15 cells/μL) but a higher proportion (16.2%) of $FOXP3^+$ cells (Treg) in the $CD4^+$ population in treatment-naïve HIV-1 patients with low CD4 (<200 cells/μL) counts than in those with high CD4 counts (34 cells/μL and 9.3%) or healthy adults (48 cells/μL and 7.5%). In HIV-1 patients, $CD45RA^+CCR7^+$, $CD45RA^-CCR7^+$, and $CD45RA^-CCR7^-$ subsets were identified in the Treg population, and the proportion of $CD45RA^-CCR7^-$ Treg was higher (57.9%) in patients with low CD4 than high CD4 counts (38.3%). Treg were in a high proliferation state especially in patients with low CD4 counts. HIV viral load correlated positively with the Treg proliferation rate and the proportion of $CD45RA^-CCR7^-$ Treg. Furthermore, the proliferation of Treg correlated positively with the $CD45RA^-CCR7^-$ Treg proportion but negatively with Treg numbers. Successful antiretroviral therapy resulted in a limited increase in Treg numbers, but their frequency was reduced in 1–2 months due to a rapid rebound of $FOXP3^-$ $CD4^+$cells. Our results suggest that HIV-activating Treg may be a reason for the high frequencies of Treg and $CD45RA^-CCR7^-$ Treg in the peripheral blood of late-stage HIV-1-infected patients.

Key words: Cell proliferation · HIV · Immune regulation · Treg

Supporting Information available online

Introduction

HIV type 1 (HIV-1) infection is characterized by a progressive loss and dysfunction of $CD4^+$ T cells [1, 2]. With regard to reduced T-cell functions, accumulating evidence suggests that the balance between the immune suppression function of natural Treg cells and the effector functions of other types of lymphoid cells influences the magnitude of immune reactions in various types of infections, e.g. those caused by *Leishmania major*, *Shistosoma mansonia*, and hepatitis C virus [3–7]. FOXP3 is not only a specific marker but also a critical lineage specification factor for Treg [8–11]. Treg are considered mainly as $CD45RA^-$ cells. However, recent studies have shown that $CD45RA^+$ cells also exist among immune-suppressing $CD25^+CTLA4^+CD4^+$ T cells in adults [12, 13].

The local interaction between Treg and other T cells plays an important role in immune suppression and the local density of Treg determines the course of immune responses to infections [4, 7, 14]. Thus, Treg can be both detrimental and beneficial to the host in response to pathogens [5, 7]. For example, in HIV-infected patients, $CD4^+CD25^+$ Treg have been reported to be proportionally increased, decreased, or highly increased in tonsils, their numbers to correlate with HIV viral load, and to exhibit suppression activity [15–23]. Furthermore, antiretroviral

Correspondence: Dr. Shinichi Oka
e-mail: oka@imcj.hosp.go.jp

therapy (ART) has been reported to have either a negative or no influence on Treg or expression of FOXP3 [18, 23]. In HIV-1-infected individuals, immunodeficiency is often considered when the CD4 cell count falls below 200 cells/μL [1]. However, to our knowledge, there is controversy or little information about the absolute number, frequency, and status of homing markers of Treg in HIV-1-infected patients especially in those with low CD4 counts and late-stage AIDS-related diseases or not on ART [24, 25]. Little is known about the dynamic changes of Treg after ART has been introduced.

It is considered that the CCR7 molecule on T cells is an essential trafficking factor for T cells homing to lymphoid tissues as well as an important marker for defining differentiation stage of T cells with CD45RA molecule [26–28].

The present study was designed to investigate Treg in late-stage HIV-1-infected patients with CD4 count <200 cells/μL and the early impact of ART on Treg. We used the chemokine receptor CCR7 and CD45RA molecules to characterize distinct population of migratory Treg.

Results

High-frequency but low absolute numbers of Treg in HIV-1 patients with low CD4 counts

In this study, we enrolled 95 HIV-1-infected patients and 21 HIV-1-negative Japanese adults as our subjects. Because most AIDS-related diseases occur in HIV-1 patients when their CD4 count decreases to below 200 cells/μL, we classified the patients into two groups, a low CD4 group with a $CD4^+$ T cell count less than 200 cells/μL and a high CD4 group with a $CD4^+$ T cell count not less than 200 cells/μL, for some comparison analysis. Table 1 lists the demographic and clinical characteristics of HIV-1-infected patients and healthy HIV-1-negative controls.

Although FOXP3 expression is considered as the best and most specific marker of Treg, some studies have reported that CD127 and CD25 could distinguish Treg [29, 30]. Accordingly, we first compared the staining of FOXP3 with CD25 and CD127 using PBMC from HIV-1-positive individuals. As shown in Supporting Information Fig. 1A and B, $CD25^+CD127^-$ were a proportion of the CD4 cells. However, gating these cells as Treg seems difficult because of the smear staining of both CD25 and CD127. However, gating FOXP3 in CD4 cells was much easier because of the clear staining of FOXP3. Furthermore, we tested the correlation of the Treg by the two classification markers. Supporting Information Fig. 1C shows a good correlation between the proportion of $FOXP3^+$ and $CD25^+$ $CD127^-$ in CD4 cells in 18 HIV-1 patients. Therefore, in the present study, we considered the $FOXP3^+CD4^+$ cells as Treg, and called $FOXP3^-CD4^+$ cells as conventional $CD4^+$ T cells (Tcon).

In the next step, we investigated the frequency and absolute number of Treg in HIV-1-infected individuals without an ART history and compared them with those of healthy Japanese adults. Figure 1A and B shows FOPX3 expression in $CD4^+$ cells. As shown in Table 2, the proportion of Treg in CD4 cells was $16.2 \pm 2.6\%$ in HIV-1 patients with a low CD4 count and

Table 1. Demographic and clinical characteristics of subjects

	Group[a]		
	A (low CD4)	B (high CD4)	H (healthy)
Characteristics			
Numbers	27	68	21
Age (years, range)	39 (21–65)	38 (21–67)	38 (21–60)
Gender (male:female)	27:0	16:1	3:4
CD4 count (cells/μL, SD)	102 (58)	383 (164)	650 (178)
LogVL (SD)	5 (0.6)	4.2 (0.7)	N/A
AIDS-related diseases[b] (*n*, %)	23 (85)	11 (16)	N/A
Months of HIV^+ (range)[c]	12.3 (0–97)	21 (0–124)	N/A
Numbers for tests			
Frequency and subsets of Treg[d]	20	39	21
Ki67 staining *versus* FOXP3[e]	11	24	5
CCR7FOXP3 *versus* CD25[f]	3	16	
CD127CD25 *versus* FOXP3[g]	6	12	

[a] Low CD4: <200 cells/μL; high CD4: ≥ 200 cells/μL.
[b] AIDS-related diseases included: candida, herpes simplex virus infection, tuberculosis, pneumocystis jirovici pneumonia, lymphoma (kaposis sarcoma), *etc.*
[c] Months between the date of the first time of consulting the hospital and the date of blood collected.
[d] Table 2 and Fig. 1.
[e] Figure 2 and Supporting Information Fig. 2.
[f] Figure 1C.
[g] Supporting Information Fig. 1.

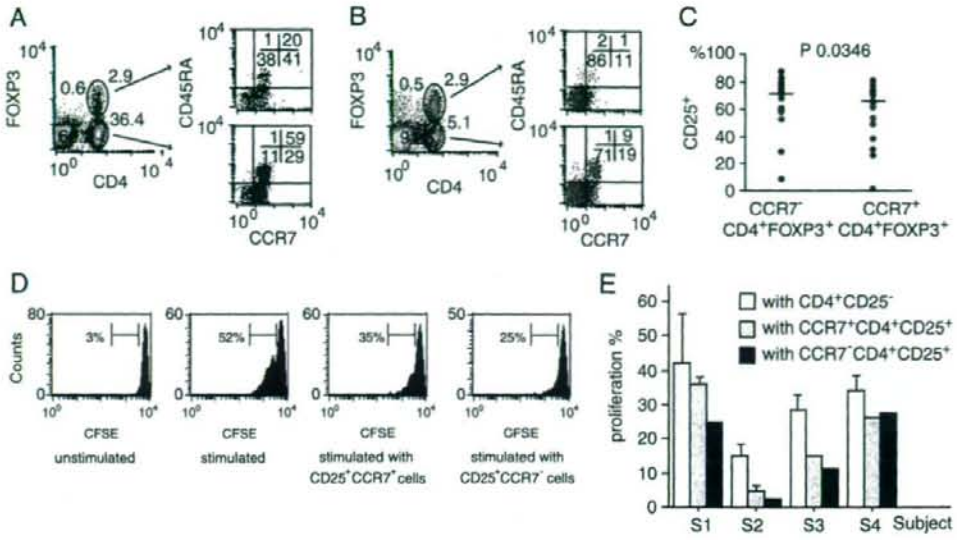

Figure 1. Subsets of Treg in healthy adults and HIV-1-infected patients. (A) Staining of a healthy adult. (B) Staining of an HIV-1-infected patient with low CD4 count. FOXP3 was mainly found in $CD4^+$ T cells both in healthy adults and HIV-1 patients. Treg ($FOXP3^+CD4^+$) cells could be subdivided into $CD45RA^+CCR7^+$, $CD45RA^-CCR7^+$, and $CD45RA^-CCR7^-$ subsets, similar to Tcon ($FOXP3^-CD4^+$, conventional CD4 cells). (C) In HIV-1 patients, the proportion of $CD25^+$ among $CCR7^-$ Treg was higher than that among $CCR7^+$ Treg ($p<0.05$, $n = 19$). (D) A representative proliferation of $CD4^+CD25^-$ responder cells cultured with $CCR7^-CD25^+CD4^+$, $CCR7^+CD25^+CD4^+$ cells, or unlabeled $CD25^-CD4^+$ cells stimulated by anti-CD3 mAb with autologous APC (the data are derived from healthy control). (E) $CCR7^+$ and $CCR7^-$ Treg suppression of responder cells in four subjects. S1–S3: healthy subjects, S4: HIV-1-positive patient (the error bars show duplicate or triplicate tests). Horizontal bars represent median values and p value represents comparison result from Wilcoxon-signed rank test.

$9.3 \pm 0.5\%$ in patients with a high CD4 count. The absolute counts of Treg in low CD4 and high CD4 groups were 15 ± 3 and 34 ± 2 cells/μL, respectively. In healthy adults, the mean CD4 count was 650 cells/μL, and the frequency of Treg among $CD4^+$ cells was $7.5 \pm 0.5\%$ with a mean absolute number of 48 ± 4 cells/μL. Therefore, HIV-1 patients with low CD4 counts had a lower absolute count but a significantly higher frequency of Treg than HIV patients with high CD4 and healthy controls.

High proportion of $CD45RA^-CCR7^-$ Treg in HIV-1 patients with low CD4

Considering the distinct homing potentials and effector functions, CD4 T cells could be subdivided into three subsets, namely naïve ($CD45RA^+CCR7^+$), central memory ($CD45RA^-CCR7^+$), and effector memory ($CD45RA^-CCR7^-$) cells, based on their surface marker and cytokine secretion [26]. Given that local interaction of Treg and Tcon plays an important role in immune suppression and the local number and/or density of Treg reflects immune suppression, we next investigated whether Treg have the same characteristic phenotype as Tcon. Figure 1A shows that Treg could be divided into three subsets, similar to Tcon, based on CD45RA and CCR7 staining in healthy controls. Interestingly, the proportion of each subset of Treg was different compared with the respective subsets of Tcon (Table 2). In healthy adults, the proportion of $CD45RA^-CCR7^-$ Treg ($39.7 \pm 2\%$) was higher than $CD45RA^-CCR7^-$ Tcon cells ($15.6 \pm 1.2\%$), but the proportion of $CD45RA^+CCR7^+$ Treg ($19.3 \pm 1.6\%$) was lower than $CD45RA^+CCR7^+$ Tcon cells ($45.8 \pm 2.4\%$).

In HIV-1-infected patients, the staining patterns of intracellular FOXP3 and surface CD4, CD45RA, and CCR7 were similar to those in healthy controls (Fig. 1A and B). Figure 1B shows a high proportion of $CD45RA^-CCR7^-$ Treg in a representative patient with a low CD4 count. As shown in Table 2, the proportion of $CD45RA^-CCR7^-$ Treg in the low CD4 group ($57.9 \pm 4.2\%$) was significantly higher than in the high CD4 ($38.3 \pm 1.8\%$) or control groups ($39.7 \pm 2\%$). In contrast, the proportion of $CD45RA^-CCR7^+$ Treg in patients with low CD4 counts was significantly lower than in those with high CD4 counts and the control groups. In all subject groups, the proportions of $CD45RA^-$ cells in Treg were higher than in Tcon. Moreover, we found that in HIV-1-infected patients, the proportion of $CD25^+$ in $CCR7^-$ Treg ($64 \pm 19\%$) was higher than in $CCR7^+$ Treg ($58.8 \pm 21\%$, Fig. 1C).

$CD45RA^+$ Treg have been reported to show suppressive function [12]. Based on the finding of a high proportion of $CCR7^-$ Treg in patients with a low CD4 count (Table 2), and considering that $CCR7^+$ cells tend to home to lymphoid tissues whereas $CCR7^-$ cells tend to move to peripheral tissues, we next investigated whether there is any difference in the suppressive activity between $CCR7^+$ and $CCR7^-$ Treg. The results showed

Table 2. Comparison of Treg and Tcon in healthy persons and HIV-1-infected patients[a)]

	Healthy (H)	HIV-1(+)ART(−)		p value		
		CD4<200 (A)	CD4≥200 (B)	A versus B	A versus H	B versus H
Number of subjects	21	20	39			
Lymphocytes (cells/μL)	1718 (381)	1028 (447)	1661 (579)	<0.0001	<0.0001	NS
CD4 (cells/μL)	650 (178)	108 (58)	395 (195)	<0.0001	<0.0001	<0.0001
CD4 (%)	38.4 (8.6)	11.4 (7.6)	20.5 (8.5)	0.0001	<0.0001	<0.0001
Treg (cells/μL)	48 (16)	15 (11)	34 (14)	<0.0001	<0.0001	0.0008
Treg (%)	7.5 (2.4)	16.2 (11.8)	9.3 (3.4)	0.0137	0.0004	0.0464
Treg (%)						
$CCR7^+$	57	40.1	59.6	0.0001	0.0029	NS
$CD45RA^+CCR7^+$	19.3	13.4	21.1	0.0109	0.0504	NS
$CD45RA^-CCR7^-$	39.7	57.9	38.3	0.0001	0.0006	NS
$CD45RA^-CCR7^+$	37.7	26.7	38.5	0.0005	0.0057	NS
$CD45RA^-$	77.4	84.6	76.8	0.0131	0.0419	NS
Tcon (%)						
$CCR7^+$	81.3	55.8	74.8	0.0178	0.0035	NS
$CD45RA^+CCR7^+$	45.8	31.9	41.1	NS	0.0217	NS
$CD45RA^-CCR7^-$	15.6	36.8	22.1	0.0283	0.0035	0.04
$CD45RA^-CCR7^+$	35.5	23.9	33.7	0.0048	0.0045	NS
$CD45RA^-$	51.1	60.7	55.8	NS	NS	NS
p Value (Treg versus Tcon)						
$CCR7^+$	<0.0001	0.0187	<0.0001			
$CD45RA^+CCR7^+$	<0.0001	0.0001	<0.0001			
$CD45RA^-CCR7^-$	<0.0001	0.0004	<0.0001			
$CD45RA^-CCR7^+$	NS	NS	0.005			
$CD45RA^-$	<0.0001	<0.0001	<0.0001			

a) Data are means (SD). NS: not significant. CD4<200, CD4≥200: 200 cells/μL. Mann–Whitney U-test was used for comparison between groups (A versus B, A versus H, B versus H). Wilcoxon-signed rank test was used for comparison in group (Treg versus Tcon).

that both $CCR7^+$ and $CCR7^-$ $CD25^+CD4^+$ cells suppressed the proliferation of responder cells (Fig. 1D). The suppressive activity was observed in three healthy controls and one HIV-1 patient (Fig. 1E), although no difference was found in the suppression function between the $CCR7^+$ and $CCR7^-$ Treg.

The above results demonstrated the existence of $CD45RA^+CCR7^+$, $CD45RA^-CCR7^+$, and $CD45RA^-CCR7^-$ Treg subsets, similar to Tcon. The proportion of $CCR7^+$ Treg was lower than $CCR7^+$ Tcon cells in both healthy controls and HIV-1 patients. However, the proportion of $CD45RA^-CCR7^-$ Treg was higher than $CD45RA^-CCR7^-$ Tcon, particularly in patients with low CD4 count.

High proliferation of Treg correlates with HIV-1 viral load

Immune cells are activated in HIV-infected patients and such activation is linked to CD4 cell depletion [31]. To determine the mechanism of the high frequency of Treg and $CD45RA^-CCR7^-$ Treg in advanced HIV patients, we stained CD4 cells for the proliferation markers Ki67 in 24 patients (including 11 patients with low CD4 counts and 13 patients with high CD4 counts) and five healthy controls. Figure 2A shows that there was no difference between gating the Ki67 in Treg and Tcon in a healthy control and an HIV-1-infected person. As shown in Fig. 2, the proportions of Ki67-stained cells among Treg in low CD4, high CD4, and control groups (41.7, 24.5, and 22.3%, respectively) were higher than those in Tcon cells (18.1, 11.8, and 7.4%, respectively) (Fig. 2B). The expression of Ki67 in both Treg and Tcon cells was higher in patients with low CD4 counts than in those with high CD4 counts and healthy controls. Furthermore, in the 24 HIV-1-infected patients assessed for Ki67, HIV-1 viral load showed a positive correlation with the frequency of Ki67 in Treg and the proportion of $CD45RA^-CCR7^-$ in Treg. However, the CD4 count showed a negative correlation with the frequency of Ki67 in Treg (Fig. 2C). Moreover, the frequency of Ki67 in Treg correlated negatively with the Treg count and the proportion of $CD45RA^+CCR7^+$ in Treg, but positively with the proportion of $CD45RA^-CCR7^-$ in Treg (Fig. 2D). The same correlation was also observed in Tcon cells (Supporting Information Fig. 2).

ART reduces the frequency of Treg

In HIV-1-infected patients, ART can effectively reduce the HIV viral load and improve CD4 counts. In highly active ART-treated patients, a depleted or normalized Treg was observed in

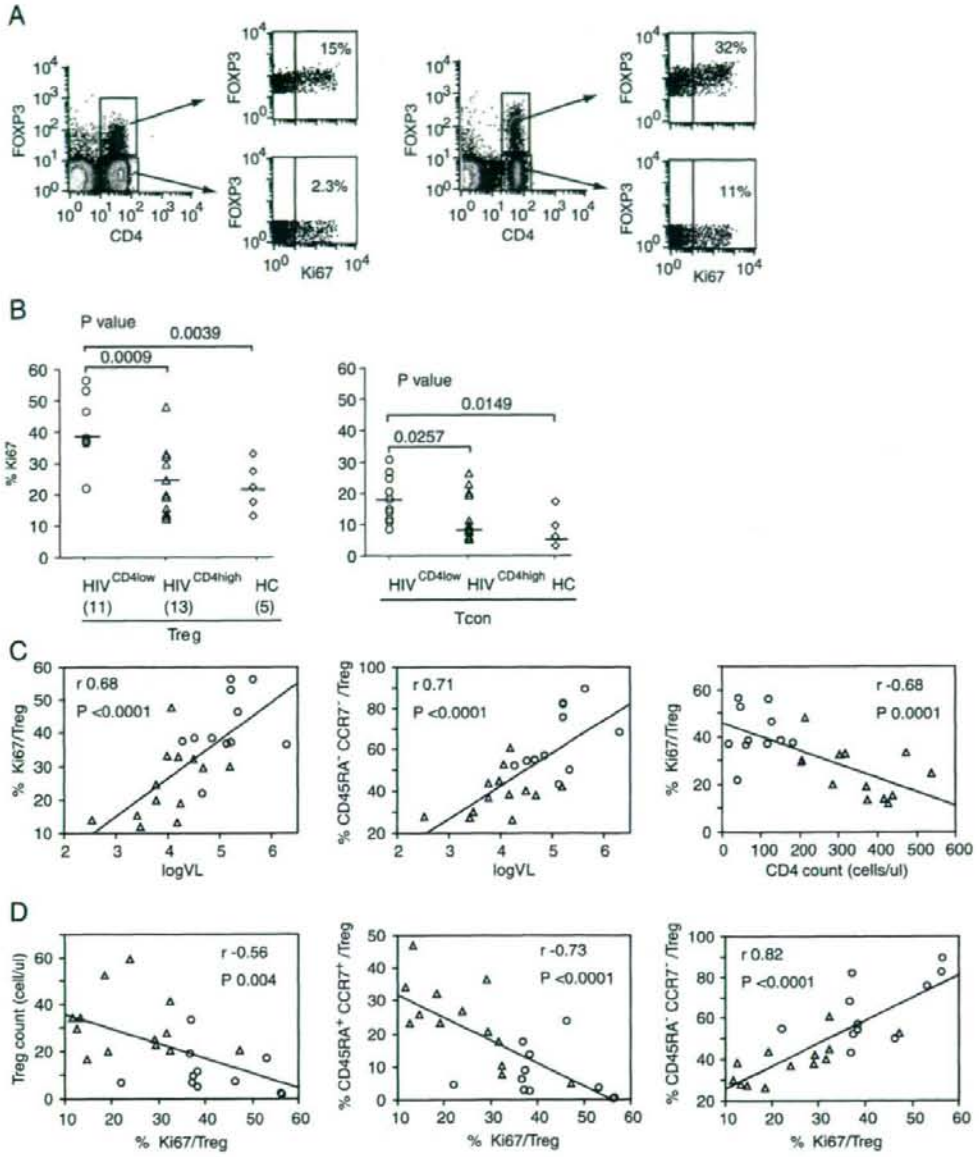

Figure 2. Ki67 staining and high proliferation rate of Treg is associated with viral load. (A) Gating of Ki67 in FOXP3$^+$ and FOXP3$^-$ CD4$^+$ cells in a healthy control (left panel) and an HIV-1-infected person (right panel). (B) Proportion of Ki67-positive Treg (left panel) is higher than that of Ki67-positive Tcon cells (right panel) in healthy controls (HC), HIV-1-infected patients with low CD4 count (HIV^{CD4low}) and HIV-1-infected patients with high CD4 count (HIV^{CD4high}) (numbers in parentheses represent the number of subjects tested). The percentages of Ki67-positive Treg and Tcon cells in the low CD4 group are higher than those in the high CD4 group and healthy control, respectively. (C) HIV-1 viral load shows a positive correlation with the percentage of Ki67 in Treg (left panel) and the proportion of CD45RA$^-$CCR7$^-$ Treg (middle panel). The CD4 count shows a negative correlation with the percentage of Ki67 in Treg (right panel). (D) The percentage of Ki67 in Treg shows correlation negatively with Treg count (left panel) and the proportion of CD45RA$^+$CCR7$^+$ Treg (middle panel) but positively with the proportion of CD45RA$^-$CCR7$^-$ Treg (right panel). Horizontal bars represent median values and p values represent results from Wilcoxon-signed rank test. Simple regression was used for correlation analysis.

PBMC and mucosal tissue [23, 32]. To investigate the impact of ART on Treg, we checked the dynamic change in Treg, their proliferation state, and subsets in nine patients until 9 months after commencement of ART (Fig. 3). The plasma viral load decreased sharply soon after commencement of ART (Fig. 3A). Associated with the decrease in viral load was a rise in the $CD4^+$ count especially in the first 2 months of ART. The CD4 count increased more than 100 cells/μL average in the first month (Fig. 3B). The absolute count of Treg increased in the first month but decreased to some extent thereafter (Fig. 3C); the frequency of Treg decreased rapidly to normal levels within 1–2 months of commencement of ART in all patients (Fig. 3D). On the other hand, the change in the proportion of Ki67 among Tcon and Treg showed a complex pattern. The proportion of Ki67 among Tcon cells increased in the first month of treatment and then decreased and fluctuated on a small scale thereafter (Fig. 3E). However, in the first 1–2 months of ART, the proportion of Ki67 among Treg decreased but maintained high levels until 9 months of ART (Fig. 3F). There was no significant change in each subset in both Treg and Tcon (Fig. 3G and H). However, the $CD45RA^-CCR7^-$ subset still accounted for a high proportion, especially in Treg (Fig. 3G and H, the right panels). The detailed change of each item in each patient is shown in Supporting Information Fig. 3. These results suggest that after initiation of ART, the slow change in the absolute number of Treg and the rapid rebound of Tcon counts resulted in a rapid normalization of the frequency of Treg in HIV-1 patients.

Discussion

Regulation of the immune response is important in maintaining self-tolerance. However, in individuals with immunodeficiency, such as patients with HIV infection, severe immune suppression may contribute to progression of AIDS. Previous studies reported activation of the immune system in HIV-1-infected patients and indicated that human $CD4^+CD25^{high}FOXP3^+$ Treg cells are derived through rapid turnover of memory populations *in vivo* [31, 33, 34].

In the present study, we found that untreated HIV-1-infected patients with low CD4 counts have a high frequency of Treg and $CD45RA^-CCR7^-$ Treg. Cell proliferation was higher in Treg than Tcon cells, especially in HIV-1 patients with low CD4 counts. In these patients, both Tcon and Treg showed a high proliferation state, particularly about 40% Treg were Ki67-positive. Ndhlovu *et al.* [22] reported that $FOXP3^+CD127^{lo}$ $CD4^+$ T cells in PBMC showed a strong negative correlation with T-cell activation during the early chronic stage of HIV infection. In our study, we also found a negative correlation between the proliferating frequency of Treg and Treg absolute count. However, we found that the proliferation of Treg correlated positively with the proportion of $CD45RA^-CCR7^-$ Treg. Furthermore, HIV viral load showed a positive correlation with both Treg proliferation and the proportion of $CD45RA^-CCR7^-$ Treg. These results suggest that HIV infection may activate Treg and result in an increased proportion of $CD45RA^-CCR7^-$ among Treg. On the other hand, Epple *et al.* [32] reported that the frequency and absolute counts of mucosal Treg were highly increased in untreated HIV patients. This finding may be considered another reason for our results because $CCR7^+$ lymphocytes tend to home to lymph nodes and lymphoid tissues. Therefore, we consider that in HIV-infected patients, HIV could simultaneously activate the differentiation of Treg as well as stimulate $CCR7^+$ Treg homing to lymph nodes and lymphoid tissues. These two effects of HIV on Treg result in the high frequency of Treg and a high proportion of $CD45RA^-CCR7^-$ Treg in peripheral blood in patients with low CD4 counts.

ART has been a great success in controlling HIV replication and aiding the recovery of CD4 T cells. However, data about its impact on Treg, especially in detail, are rare. In the current study, we observed that with the rapid decrease in viral load was a robust rebound of Tcon 1–2 months after ART initiation; however, the number of Treg increased in some patients but was almost unchanged in others. The unbalanced change in Tcon and Treg resulted in the frequency of Treg decreasing precipitously to normal levels in the first 1–2 months of therapy. Although the viral load decreased to a very low level in a short period after ART introduction, the proliferative state of Tcon and Treg did not decrease significantly. On the contrary, both Tcon and Treg maintained a high proliferation level, especially Treg. Moreover, the three subsets, *i.e.* $CD45RA^+CCR7^+$, $CD45RA^-CCR7^+$, and $CD45RA^-CCR7^-$ in Tcon and Treg did not show a robust change till 9 months. The results suggest that the recovery of phenotypes needs a much longer period, even if they can recover after ART.

Chase *et al.* [23] observed Treg depletion in highly active ART-treated HIV-1 patients but not in elite suppressors. Here, we did not observe depletion of Treg counts after ART introduction, but we indeed noticed a rapid normalization of the Treg frequency. As we know, to do the suppression assay *in vitro*, an appropriate ratio of Treg to responder cells is needed for observing significant suppression. Considering the suppressive function of both $CCR7^+$ and $CCR7^-$ Treg, we think that the high frequency of Treg, but not the low absolute number of Treg, provides a much better suppressive marker in treatment-naïve HIV-1 patients with low CD4 counts. On the other hand, ART may induce some improvement of the immune suppression because it could reduce the frequency of Treg.

In summary, our results of high frequencies of Treg and $CD45RA^-CCR7^-$ Treg, which tend to migrate to non-lymphoid tissues, in untreated HIV-1 patients with low CD4 counts, emphasize the potential role of Treg in immune deficiency in late-stage HIV-1 infection. Furthermore, anti-HIV treatment could result in a rapid rebound of conventional T cells but not a robust improvement of Treg within 9 months after ART initiation. The different response of Treg and Tcon to ART leads to a rapid decrease in the frequency of Treg. Recently, immune reconstitution syndrome (IRS) is becoming an important problem in HIV treatment. Most IRS occurs in 1–3 months after commencement

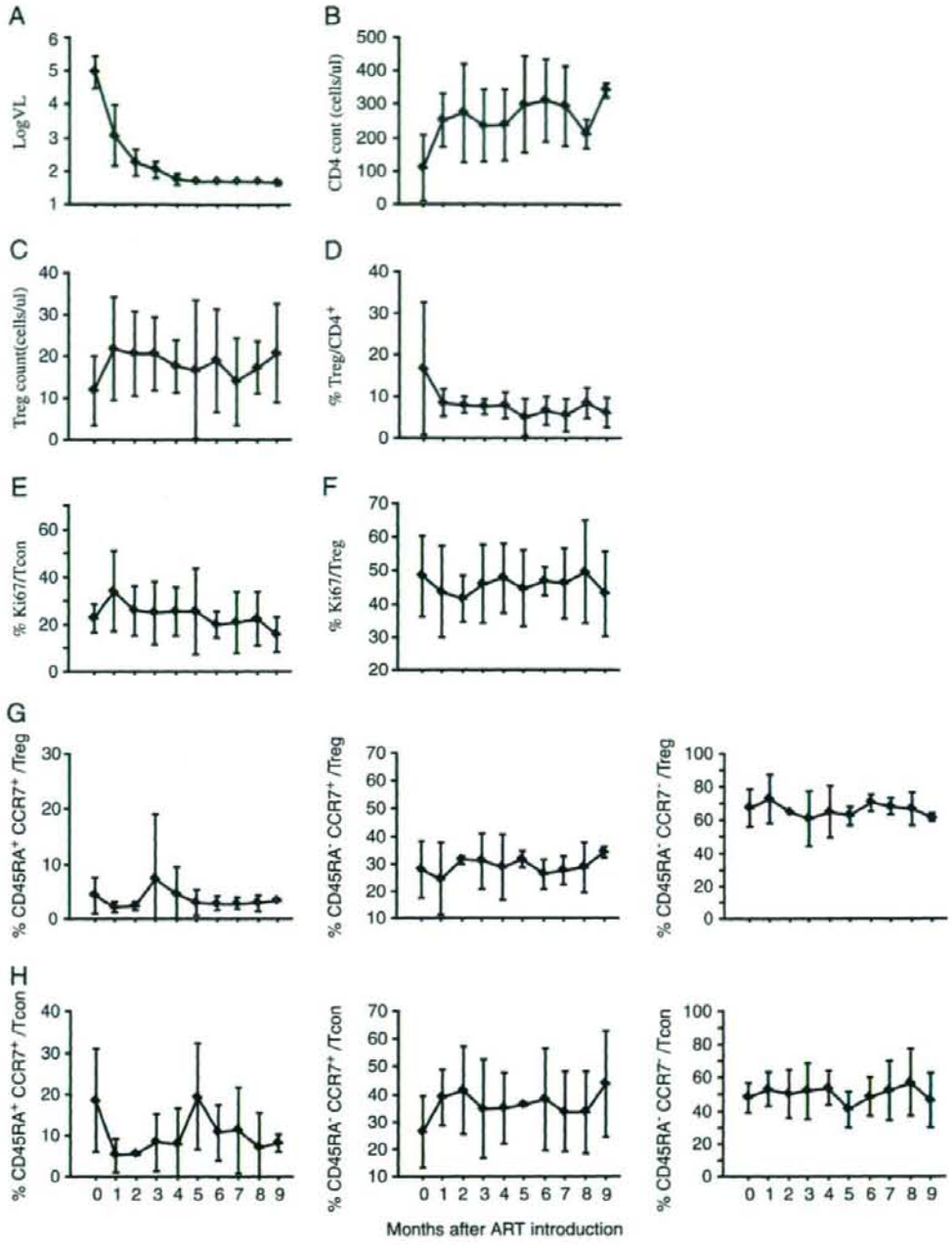

Figure 3. Serial changes in Treg and Tcon cells after commencement of ART. Commencement of ART resulted in rapid reduction in HIV viral load (A) and increase in $CD4^+$ cell count (B). Treatment caused increase in the absolute number of Treg in the first month, then fluctuated slightly thereafter (C), but resulted in a sharp decrease in their percentages in 1 month (D). The proportion of Ki67-positive Tcon increased in the first month but decreased in some extent thereafter (E), while the proportion of Ki67-positive Treg showed some change but still retained a high level at 9 months of commencement of ART (F). At 9 months after ART started, the recovery of the proportion of $CD45RA^+CCR7^+$ Treg (G, left panel) and Tcon (H, left panel) seems very slow, while the proportion of $CD45RA^-CCR7^+$ Treg (G, middle panel) and Tcon (H, middle panel) increased in some extent. However, the proportion of $CD45RA^-CCR7^-$ Treg (G, right panel) and $CD45RA^-CCR7^-$ Tcon (H, right panel) showed a small-scale change, but $CD45RA^-CCR7^-$ Treg maintained a high proportion till 9 months. (A–F) was from nine patients, while (G–H) was from six of them. Vertical bars represent mean ± 1SD.

of ART. Thus, we suppose that the unbalanced improvement of conventional CD4 cells and Treg after commencement of ART might be a factor for IRS. However, this issue needs more investigation.

Materials and methods

Subjects

The subjects were 95 HIV-1-infected patients who have not received any ART and gave written consent before enrollment in this study at the AIDS Clinical Center, International Medical Center of Japan, Tokyo. Nine patients who started ART were followed up for investigation of the impact of ART on Treg. Twenty-one HIV-1-negative adults were recruited as healthy controls. The demographic and clinical characteristics of the subjects are listed in Table 1. HIV-1 viral load was quantified by AMPLICOR HIV-1 MONITOR Test (Roche Diagnostics).

Cell preparation

PBMC were prepared from blood samples collected into EDTA-containing tubes by Ficoll-paque gradient centrifugation. Ki67 staining and evaluation of the ART-treated patients were carried out using cryopreserved PBMC.

For suppression assay, $CD4^+$ cells were isolated from freshly prepared PBMC by using $CD4^+$ T-cell Isolation Kit (Miltenyi Biotec, Bergisch Gladbach, Germany) according to instructions provided by the manufacturer. $CD4^+$ cells were separated by anti-CD25 mAb (PE) and anti-PE Multisort Kit (Miltenyi) into $CD25^-$ and $CD25^+$ cells. After microbeads release, $CD25^+$ cells were sorted into $CCR7^+$ and $CCR7^-$ cells by using anti-CCR7 mAb (FITC, mouse IgG2a, R&D Systems, Minneapolis, MN) and Rat Anti-Mouse IgG2a+b Microbeads (Miltenyi). The $CD4^+CD25^-$ cells were labeled by 2 μM 5-6-CFSE as responder cells in the suppression assay. Unlabeled $CD4^+CD25^-$ cells were used as non-Treg for cell number control. PBMC that were depleted of $CD3^+$ cells by CD3 MicroBeads (Miltenyi) and irradiated with 3000 rad were used as APC.

Cell staining and flow cytometry

Freshly isolated PBMC were surface stained and also stained intracellularly for FOXP3 (PE/APC labeled, clone PCH101, eBioscience, San Diego, CA) and other markers. The stained cells were analyzed on Becton Dickinson FACSCalibur with CellQuest software (BD Bioscience, San Jose, CA). The monoclonal antibodies used in these staining procedures included anti-CCR7-FITC, anti-CD4-perCP, anti-CD25-PE, anti-CD45RA-APC/perCP, anti-Ki67-PE (BD PharMingen, San Diego, CA), and anti-CD127-FITC (eBioscience).

In vitro suppression assay

In a 96-well, round-bottom plate coated with anti-CD3 mAb (0.25–0.5 μg/mL), 5×10^4 CFSE-labeled $CD4^+CD25^-$ cells were seeded and followed by adding autologous APC (2.5×10^4). For testing Treg suppression, the same number of $CD4^+CD25^+$ $CCR7^+$ or $CCR7^-$ cells was added as regulatory cells. In control wells, the same number of unlabeled non-Treg $CD4^+CD25^-$ cells was added in order to adjust cell numbers in each well. After 3–4 days culture in an incubator at 37°C under 5% CO_2, the cells were harvested and analyzed on FACSCalibur. Live cells were gated and the dilution of CFSE was measured as proliferation of responder cells.

Statistical analysis

Data are expressed as mean ± SD. Differences between groups or stratified groups were examined for statistical significance using Mann–Whitney *U*-test and Wilcoxon-signed rank test. Simple linear regression was used for correlation analysis. All analyses were conducted using the StatView software (version 5.0). A p value of <0.05 was considered statistically significant.

Acknowledgements: We are grateful to Dr. Yoshimi Kikuchi, Tsunefusa Hayashida, Dr. Kiyoto Tsuchiya, and the entire staff of the AIDS Clinical Center, International Medical Center of Japan for their help and cooperation. We thank Dr. F.G. Issa, Word-Medex Pty Ltd., Sydney, Australia for English editing. This work was supported by a grant-in-aid for AIDS research from the Ministry of Health, Labor, and Welfare of Japan, and by the Japanese Foundation of AIDS Prevention (X.Bi).

Conflict of interest: The authors declare no financial or commercial conflict of interest.

References

1 **Douek, D. C., Picker, L. J. and Koup, R. A.**, T cell dynamics in HIV-1 infection. *Annu. Rev. Immunol.* 2003. **21**: 265–304.

2 **Gandhi, R. T. and Walker, B. D.**, Immunologic control of HIV-1. *Annu. Rev. Med.* 2002. **53**: 149–172.

3 **Sakaguchi, S., Sakaguchi, N., Asano, M., Itoh, M. and Toda, M.**, Immunologic self-tolerance maintained by activated T cells expressing IL-2 receptor alpha-chains (CD25). Breakdown of a single mechanism of self-tolerance causes various autoimmune diseases. *J. Immunol.* 1995. **155**: 1151–1164.

4 **Mills, K. H.**, Regulatory T cells: friend or foe in immunity to infection? *Nat. Rev. Immunol.* 2004. **4**: 841–855.

5 **Rouse, B. T., Sarangi, P. P. and Suvas, S.**, Regulatory T cells in virus infections. *Immunol. Rev.* 2006. **212**: 272–286.

6 **Klenerman, P. and Hill, A.,** T cells and viral persistence: lessons from diverse infections. *Nat. Immunol.* 2005. **6**: 873–879.

7 **Belkaid, Y. and Rouse, B. T.,** Natural regulatory T cells in infectious disease. *Nat. Immunol.* 2005. **6**: 353–360.

8 **Coffer, P. J. and Burgering, B. M.,** Forkhead-box transcription factors and their role in the immune system. *Nat. Rev. Immunol.* 2004. **579**: 191–198.

9 **Fontenot, J. D., Rasmussen, J. P., Williams, L. M., Dooley, J. L., Farr, A. G. and Rudensky, A. Y.,** Regulatory T cell lineage specification by the forkhead transcription factor Foxp3. *Immunity* 2005. **22**: 329–341.

10 **Sakaguchi, S.,** Naturally arising Foxp3-expressing CD25+CD4+ regulatory T cells in immunological tolerance to self and non-self. *Nat. Immunol.* 2005. **6**: 345–352.

11 **Wu, Y., Borde, M., Heissmeyer, V., Feuerer, M., Lapan, A. D., Stroud, J. C., Bates, D. L. et al.,** FOXP3 controls regulatory T cell function through cooperation with NFAT. *Cell* 2006. **126**: 375–387.

12 **Seddiki, N., Santner-Nanan, B., Tangye, S. G., Alexander, S. I., Solomon, M., Lee, S., Nanan, R. and de Saint Groth, B. F.,** Persistence of naive CD45RA$^+$ regulatory T cells in adult life. *Blood* 2006. **107**: 2830–2838.

13 **Thornton, C. A., Upham, J. W., Wikstrom, M. E., Holt, B. J., White, G. P., Sharp, M. J., Sly, P. D. and Holt, P. G.,** Functional maturation of CD4$^+$CD25$^+$ CTLA4$^+$CD45RA$^+$ T regulatory cells in human neonatal T cell responses to environmental antigens/allergens. *J. Immunol.* 2004. **173**: 3084–3092.

14 **Bacchetta, R., Passerini, L., Gambineri, E., Dai, M., Allan, S. E., Perroni, L., Dagna-Bricarelli, F. et al.,** Defective regulatory and effector T cell functions in patients with FOXP3 mutations. *J. Clin. Invest.* 2006. **116**: 1713–1722.

15 **Tsunemi, S., Iwasaki, T., Imado, T., Higasa, S., Kakishita, E., Shirasaka, T. and Sano, H.,** Relationship of CD4$^+$CD25$^+$ regulatory T cells to immune status in HIV- infected patients. *AIDS* 2005. **19**: 879–886.

16 **Aandahl, E. M., Michaelsson, J., Moretto, W. J., Hecht, F. M. and Nixon, D. F.,** Human CD4$^+$ CD25$^+$ regulatory T cells control T-cell responses to human immunodeficiency virus and cytomegalovirus antigens. *J. Virol.* 2004. **78**: 2454–2459.

17 **Eggena, M. P., Barugahare, B., Jones, N., Okello, M., Mutalya, S., Kityo, C., Mugyenyi, P. and Cao, H.,** Depletion of regulatory T cells in HIV infection is associated with immune activation. *J. Immunol.* 2005. **174**: 4407–4414.

18 **Weiss, L., Donkova-Petrini, V., Caccavelli, L., Balbo, M., Carbonneil, C. and Levy, Y.,** Human immunodeficiency virus-driven expansion of CD4$^+$ CD25$^+$ regulatory T cells, which suppress HIV-specific CD4 T-cell responses in HIV-infected patients. *Blood* 2004. **104**: 3249–3256.

19 **Kinter, A. L., Hennessey, M., Bell, A., Kern, S., Lin, Y., Daucher, M., Planta, M. et al.,** CD25(+)CD4(+) regulatory T cells from the peripheral blood of asymptomatic HIV-infected individuals regulate CD4(+) and CD8(+) HIV-specific T cell immune responses *in vitro* and are associated with favorable clinical markers of disease status. *J. Exp. Med.* 2004. **200**: 331–343.

20 **Andersson, J., Boasso, A., Nilsson, J., Zhang, R., Shire, N. J., Lindback, S., Shearer, G. M. and Chougnet, C. A.,** The prevalence of regulatory T cells in lymphoid tissue is correlated with viral load in HIV-infected patients. *J. Immunol.* 2005. **174**: 3143–3147.

21 **Krathwohl, M. D., Schacker, T. W. and Anderson, J. L.,** Abnormal presence of semimature dendritic cells that induce regulatory T cells in HIV-infected subjects. *J. Infect. Dis.* 2006. **193**: 494–504.

22 **Ndhlovu, L. C., Loo, C. P., Spotts, G., Nixon, D. F. and Hecht, F. M.,** FOXP3 expressing CD127lo CD4$^+$T cells inversely correlate with CD38$^+$CD8$^+$ T cell activation level in primary HIV-1 infection. *J. Leukoc. Biol.* 2008. **83**: 254–262.

23 **Chase, A. J., Yang, H., Zhang, H., Blankson, J. N. and Siliciano, R. F.,** Preservation of FOXP3$^+$ regulatory T cells in the peripheral blood of HIV-1-infected elite suppressors correlates with low CD4$^+$ T-cell activation. *J. Virol.* 2008. **82**: 8307–8315.

24 **de St Groth, B. F. and Landay, A. L.,** Regulatory T cells in HIV infection: pathogenic or protective participants in the immune response? *AIDS* 2008. **22**: 671–683.

25 **Keynan, Y., Card, C. M., Mclaren, P. J., Dawood, M. R., Kasper, K. and Fowke, K. R.,** The role of regulatory T cells in chronic and acute infections. *Clin. Infect. Dis.* 2008. **46**: 1046–1052.

26 **Sallusto, F., Lenig, D., Forster, R., Lipp, M. and Lanzavecchia, A.,** Two subsets of memory T lymphocytes with distinct homing potentials and effector functions. *Nature* 1999. **401**: 708–712.

27 **Lim, H. W., Broxmeyer, H. E. and Kim, C. H.,** Regulation of trafficking receptor expression in human forkhead box P3+regulatory T cells. *J. Immunol.* 2006. **177**: 840–851.

28 **Wei, S., Kryczek, I. and Zou, W.,** Regulatory T-cell compartmentalization and trafficking. *Blood* 2006. **108**: 426–431.

29 **Seddiki, N., Santner-Nanan, B., Martinson, J., Zaunders, J., Sasson, S., Landay, A., Solomon, M. et al.,** Expression of interleukin (IL)-2 and IL-7 receptors discriminates between human regulatory and activated T cells. *J. Exp. Med.* 2006. **203**: 1693–1700.

30 **Liu, W., Putnam, A. L., Xu-Yu, Z., Szot, G. L., Lee, M. R., Zhu, S., Gottlieb, P. A. et al.,** CD127 expression inversely correlates with FoxP3 and suppressive function of human CD4$^+$Treg cells. *J. Exp. Med.* 2006. **203**: 1701–1711.

31 **Sousa, A. E., Carneiro, J., Meier-Schellersheim, M., Grossman, Z. and Victorino, R. M.,** CD4 T cell depletion is linked directly to immune activation in the pathogenesis of HIV-1 and HIV-2 but only indirectly to the viral load. *J. Immunol.* 2002. **169**: 3400–3406.

32 **Epple, H. J., Loddenkemper, C., Kunkel, D., Troger, H., Maul, J., Moos, V., Berg, E. et al.,** Mucosal but not peripheral FOXP3$^+$ regulatory T cells are highly increased in untreated HIV infection and normalize after suppressive HAART. *Blood* 2006. **108**: 3072–3078.

33 **Hazenberg, M. D., Stuard, J. W., Otto, S. A., Borleffs, J. C., Boucher, C. A., de Boer, R. J., Miedema, F. and Hamann, D.,** T-cell division in human immunodeficiency virus (HIV)-1 infection is mainly due to immune activation: a longitudinal analysis in patients before and during highly active antiretroviral therapy (HAART). *Blood* 2000. **95**: 249–255.

34 **Vukmanovic-Stejic, M., Zhang, Y., Cook, J. E., Fletcher, J. M., McQuaid, A., Masters, J. E., Rustin, M. H. et al.,** Human CD4$^+$ CD25^{hi} Foxp3$^+$ regulatory T cells are derived by rapid turnover of memory populations *in vivo*. *J. Clin. Invest.* 2006. **116**: 2423–2433.

Abbreviations: **ART:** antiretroviral therapy · **HIV-1:** HIV type 1 · **IRS:** immune reconstitution syndrome · **Tcon:** conventional CD4$^+$ T cells

Full correspondence: Dr. Shinichi Oka, AIDS Clinical Center, International Medical Center of Japan, 1-21-1, Toyama, Shinjuku-ku, Tokyo 162-8655, Japan
Fax: +1-81-3-5273-5193
e-mail: oka@imcj.hosp.go.jp

Supporting Information for this article is available at www.wiley-vch.de/contents/jc_2040/2008/38667_s.pdf

Received: 1/7/2008
Revised: 29/9/2008
Accepted: 29/10/2008

ANTIMICROBIAL AGENTS AND CHEMOTHERAPY, Mar. 2009, p. 997–1006 Vol. 53, No. 3
0066-4804/09/$08.00+0 doi:10.1128/AAC.00689-08

GRL-02031, a Novel Nonpeptidic Protease Inhibitor (PI) Containing a Stereochemically Defined Fused Cyclopentanyltetrahydrofuran Potent against Multi-PI-Resistant Human Immunodeficiency Virus Type 1 In Vitro▽

Yasuhiro Koh,[1] Debananda Das,[2] Sofiya Leschenko,[3] Hirotomo Nakata,[1,2] Hiromi Ogata-Aoki,[1] Masayuki Amano,[1] Maki Nakayama,[1] Arun K. Ghosh,[3] and Hiroaki Mitsuya[1,2]*

Departments of Hematology and Infectious Diseases, Kumamoto University Graduate School of Medical and Pharmaceutical Sciences, Kumamoto 860-8556, Japan[1]; Experimental Retrovirology Section, HIV and AIDS Malignancy Branch, National Cancer Institute, National Institutes of Health, Bethesda, Maryland 20892[2]; and Departments of Chemistry and Medicinal Chemistry, Purdue University, West Lafayette, Indiana 47907[3]

Received 27 May 2008/Returned for modification 8 August 2008/Accepted 16 October 2008

We generated a novel nonpeptidic protease inhibitor (PI), GRL-02031, by incorporating a stereochemically defined fused cyclopentanyltetrahydrofuran (Cp-THF) which exerted potent activity against a wide spectrum of human immunodeficiency virus type 1 (HIV-1) isolates, including multidrug-resistant HIV-1 variants. GRL-02031 was highly potent against laboratory HIV-1 strains and primary clinical isolates, including subtypes A, B, C, and E (50% effective concentration [EC_{50}] range, 0.015 to 0.038 μM), with minimal cytotoxicity (50% cytotoxic concentration, >100 μM in $CD4^+$ MT-2 cells), although it was less active against two HIV-2 strains (HIV-2_{ERO} and HIV-2_{ROD}) (EC_{50}, ~0.60 μM) than against HIV-1 strains. GRL-02031 at relatively low concentrations blocked the infection and replication of each of the HIV-1_{NL4-3} variants exposed to and selected by up to 5 μM of saquinavir, amprenavir, indinavir, nelfinavir, or ritonavir and 1 μM of lopinavir or atazanavir (EC_{50} range, 0.036 to 0.14 μM). GRL-02031 was also potent against multi-PI-resistant clinical HIV-1 variants isolated from patients who had no response to the conventional antiretroviral regimens that then existed, with EC_{50}s ranging from 0.014 to 0.042 μM (changes in the EC_{50}s were less than twofold the EC_{50} for wild-type HIV-1). Upon selection of HIV-1_{NL4-3} in the presence of GRL-02031, mutants carrying L10F, L33F, M46I, I47V, Q58E, V82I, I84V, and I85V in the protease-encoding region and G62R (within p17), L363M (p24-p2 cleavage site), R409K (within p7), and I437T (p7-p1 cleavage site) in the *gag*-encoding region emerged. GRL-02031 was potent against a variety of HIV-1_{NL4-3}-based molecular infectious clones containing a single primary mutation reported previously or a combination of such mutations, although it was slightly less active against HIV-1 variants containing consecutive amino acid substitutions: M46I and I47V or I84V and I85V. Structural modeling analysis demonstrated a distinct bimodal binding of GRL-02031 to protease, which may provide advantages to GRL-02031 in blocking the replication of a wide spectrum of HIV-1 variants resistant to PIs and in delaying the development of resistance of HIV-1 to GRL-02031. The present data warrant the further development of GRL-02031 as a potential therapeutic agent for the treatment of infections with primary and multidrug-resistant HIV-1 variants.

The currently available combination therapy or highly active antiretroviral therapy (HAART) with two or more reverse transcriptase inhibitors and protease inhibitors (PIs) for human immunodeficiency virus (HIV) type 1 (HIV-1) infection and AIDS has been shown to suppress the replication of HIV-1 and extend the life expectancy of HIV-1-infected individuals (35, 38). However, the ability to provide effective long-term antiretroviral therapy for HIV-1 infection has become a complex issue, since those who initially achieved favorable viral suppression to undetectable levels have experienced treatment failure (11, 18, 28). In addition, it is evident that with these anti-HIV drugs, only partial immunologic reconstitution is attained in patients with advanced HIV-1 infection.

Nevertheless, recent analyses have revealed that the life expectancy of HIV-infected patients treated with HAART increased between 1996 and 2005, that the mortality rates for HIV-infected persons have become much closer to general mortality rates since the introduction of HAART, and that first-line HAART with boosted PI-based regimens results in less resistance within and across drug classes (2, 3, 18, 46).

In the development of new anti-HIV-1 therapeutics, we have faced a variety of challenges different from those faced during the design of the first-line drugs (7, 10, 39). The issue of the emergence of drug-resistant HIV-1 variants is one of the most formidable challenges in the era of HAART. Indeed, it is of note that the very features that contribute to the specificities and the efficacies of reverse transcriptase inhibitors and PIs provide the virus with a strategy to develop resistance (15, 19, 35), and it seems inevitable that this resistance issue will remain problematic for many years to come, although a few recently developed drugs, such as darunavir (DRV) and tipranavir, have been relatively successful as treatments for individuals carrying multidrug-resistant HIV-1 variants (5, 20).

In particular, a number of studies indicate that cross-resis-

* Corresponding author. Mailing address: Department of Hematology, Kumamoto University Graduate School of Medicine, 1-1-1 Honjo, Kumamoto 860-8556, Japan. Phone: (81) 96-373-5156. Fax: (81) 96-363-5265. E-mail: hmitsuya@helix.nih.gov.

▽ Published ahead of print on 27 October 2008.

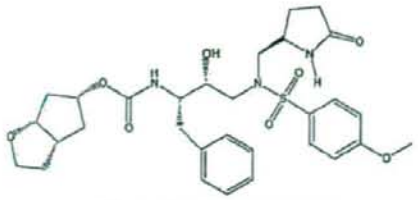

FIG. 1. Structure of GRL-02031.

tance is a major obstacle to antiviral therapy with PIs (19, 24). Obviously, the emergence of viral resistance, difficulties with compliance with the complicated treatment protocols, and adverse side effects urge the development of new classes of PIs (i) that have potent activities against existing resistant HIV-1 variants and that do not allow or delay the emergence of resistance, (ii) that have improved pharmacokinetics parameters in humans, and (iii) that have less severe side effects (43).

The present paper represents the first demonstration of the results of antiviral analyses of a novel PI which contains cyclopentanyltetrahydrofuran (Cp-THF) and which is highly potent against a wide spectrum of HIV isolates, including a variety of multi-PI-resistant clinical strains, in vitro. In addition, we selected GRL-02031-resistant HIV-1 variants in vitro and characterized their virological properties and susceptibilities to other PIs. We also demonstrated that the emergence of HIV-1 variants resistant to GRL-02031 requires multiply accumulated amino acid substitutions in the protease-encoding region. Moreover, in an attempt to explain why GRL-02031 can exert potent activity against a wide spectrum of HIV-1 variants resistant to multiple PIs, we performed structural modeling and molecular docking and examined the interactions of GRL-02031 with HIV-1 protease.

MATERIALS AND METHODS

Cells and viruses. MT-2 and MT-4 cells were grown in RPMI 1640-based culture medium supplemented with 10% fetal calf serum (JRH Biosciences, Lenexa, MD), 50 U/ml penicillin, and 50 μg/ml of streptomycin. The following HIV-1 strains were employed for the drug susceptibility assay (see below): HIV-1_{LAI}, HIV-$1_{Bs\text{-}L}$, HIV-1_{JRFL}, HIV-$1_{NL4\text{-}3}$, HIV-2_{EHO}, and HIV-2_{ROD}; two clinical HIV-1 strains isolated from drug-naive patients with AIDS, HIV-$1_{ER5ID4pre}$ and HIV-1_{MOKW} (30, 45); and seven HIV-1 clinical isolates which were originally isolated from patients with AIDS who had received 9 to 11 anti-HIV-1 drugs over the past 32 to 83 months and which were genotypically and phenotypically characterized as multi-PI-resistant HIV-1 variants (47, 48). HIV-$1_{92UG037}$, HIV-$1_{97ZA003}$, and HIV-$1_{92TH019}$ were obtained from the NIH AIDS Reagent Program. All primary HIV-1 strains were passaged once or twice in 3-day-old phytohemagglutinin-activated peripheral blood mononuclear cells (PHA-PBMs), and the culture supernatants were stored at −80°C until use.

Antiviral agents. GRL-02031 (Fig. 1), a novel nonpeptidic PI containing Cp-THF, was designed and synthesized. Detailed methods for the synthesis of GRL-02031 will be described elsewhere by A. K. Ghosh et al. 3′-Azido-2′,3′-dideoxythymidine (AZT; zidovudine) was purchased from Sigma (St. Louis, MO). Saquinavir (SQV) and ritonavir (RTV) were kindly provided by Roche Products Ltd. (Welwyn Garden City, United Kingdom) and Abbott Laboratories (Abbott Park, IL), respectively. Amprenavir (APV) was a kind gift from Glaxo-Wellcome, Research Triangle Park, NC. Nelfinavir (NFV) and indinavir (IDV) were kindly provided by Japan Energy Inc, Tokyo, Japan. Lopinavir (LPV) was synthesized by previously published methods (48). Atazanawir (ATV) was a kind gift from Bristol-Myers Squibb (New York, NY).

Drug susceptibility assay. The susceptibilities of HIV-1_{LAI}, HIV-$1_{Bs\text{-}L}$, HIV-2_{EHO}, HIV-2_{ROD}, and the primary HIV-1 isolates to various drugs were determined as described previously (26), with minor modifications. Briefly, MT-2 cells (2×10^4/ml) were exposed to 100 50% tissue culture infectious dose ($TCID_{50}$s) of HIV-1_{LAI}, HIV-$1_{Bs\text{-}L}$, HIV-2_{EHO}, or HIV-2_{ROD} in the presence or the absence of various concentrations of drugs in 96-well microculture plates; and the plates were incubated at 37°C for 7 days. After 100 μl of the medium was removed from each well, 3-(4,5-dimetylthiazol-2-yl)-2,5-diphenyltetrazolium bromide (MTT) solution (10 μl, 7.5 mg/ml in phosphate-buffered saline) was added to each well in the plate, followed by incubation at 37°C for 2 h. After incubation, to dissolve the formazan crystals, 100 μl of acidified isopropanol containing 4% (vol/vol) Triton X-100 was added to each well and the optical density was measured in a kinetic microplate reader (Vmax; Molecular Devices, Sunnyvale, CA). All assays were performed in duplicate or triplicate.

To determine the sensitivities of the primary HIV-1 isolates to drugs, PHA-PBMs (10^6/ml) were exposed to 50 $TCID_{50}$s of each primary HIV-1 isolate and cultured in the presence or the absence of various concentrations of drugs in 10-fold serial dilutions in 96-well microculture plates. To determine the drug susceptibilities of certain laboratory HIV-1 strains, MT-4 cells were employed as target cells, as described previously (26), with minor modifications. In brief, MT-4 cells (10^5/ml) were exposed to 100 $TCID_{50}$s of drug-resistant IIIV-1 strains in the presence or the absence of various concentrations of drugs and were incubated at 37°C. On day 7 of culture, the supernatants were harvested and the amounts of the p24 Gag protein were determined by using a fully automated chemiluminescent enzyme immunoassay system (Lumipulse F; Fujirebio Inc., Tokyo, Japan) (29). The drug concentrations that suppressed the production of p24 Gag protein by 50% (EC_{50}) were determined by comparison of the amount of p24 Gag protein produced in drug-treated cell cultures with the level of p24 Gag protein produced in a drug-free control cell culture. All assays were performed in triplicate.

Generation of PI-resistant HIV-1 variants in vitro. MT-4 cells (10^5/ml) were exposed to HIV-$1_{NL4\text{-}3}$ (500 $TCID_{50}$s) and cultured in the presence of various PIs at an initial concentration of 0.01 to 0.03 μM. Viral replication was monitored by determination of the amount of p24 Gag produced by MT-4 cells. The culture supernatants were harvested on day 7 and were used to infect fresh MT-4 cells for the next round of culture in the presence of increasing concentrations of each drug. When the virus began to propagate in the presence of the drug, the drug concentration was generally increased two- to threefold. Proviral DNA samples obtained from the lysates of infected cells were subjected to nucleotide sequencing. This drug selection procedure was carried out until the drug concentration reached 5 μM.

Determination of nucleotide sequences. Molecular cloning and determination of the nucleotide sequences of HIV-1 isolates passaged in the presence of anti-HIV-1 agents were performed as described previously (26, 47). In brief, high-molecular-weight DNA was extracted from HIV-1-infected MT-4 cells by using the InstaGene matrix (Bio-Rad Laboratories, Hercules, CA) and was subjected to molecular cloning, followed by sequence determination. The primers used for the first round of PCR of the entire Gag- and protease-encoding regions of the HIV-1 genome were LTR-F1 (5′-GAT GCT ACA TAT AAG CAG CTG C-3′) and PR12 (5′-CTC GTG ACA AAT TTC TAC TAA TGC-3′). The first-round PCR mixture consisted of 5 μl of proviral DNA solution, 2.0 U of Premix *Taq* (Ex *Taq* version; Takara Bio Inc., Otsu, Japan), and 12.5 pmol of each of the first-round PCR primers in a total volume of 50 μl. The PCR conditions employed were as follows: an initial 2 min at 94°C, followed by 35 cycles of 30 s at 94°C, 30 s at 58°C, and 3 min at 72°C, with a final 8-min extension at 72°C. The first-round PCR products (1 μl) were used directly in the second round of PCR with primers LTR-F2 (5′-GAG ACT CTG GTA ACT AGA GAT C-3′) and Ksma2.1 (5′-CCA TCC CGG GCT TTA ATT TTA CTG GTA C-3′) under the same PCR conditions described above. The second-round PCR products were purified with spin columns (MicroSpin S-400 HR columns; Amersham Biosciences Corp., Piscataway, NJ), cloned directly, and subjected to sequencing with an ABI model 377 automated DNA sequencer (Applied Biosystems, Foster City, CA). The viral RNA in the selection culture should contain a number of noninfectious (or dead) virions due to randomly occurring amino acid substitutions, which could provide misleading results if the sequences of such noninfectious or dead virions were erroneously taken into account. The viral DNA extracted from the newly infected cells in the present cell-free transmission system represents the infectious virions in the previous culture.

Generation of recombinant HIV-1 clones. The PCR products obtained as described above were digested with two enzymes, ApaI and SmaI; and the fragments obtained were introduced into pHIV-1_{NLSma}, designed to have a SmaI site by changing two nucleotides (2590 and 2593) of pHIV-$1_{NL4\text{-}3}$, as described previously (14, 25). To generate HIV-1 clones carrying the desired mutations, site-directed mutagenesis was performed with a QuikChange site-directed mutagenesis kit (Stratagene, La Jolla, CA), and the mutation-containing genomic fragments were introduced into pHIV-1_{NLSma}. Determination of the nucleotide

TABLE 1. Antiviral activity of GRL-02031 against HIV-1_{LAI}[a]

Compound	EC_{50} (μM)	CC_{50}(μM)	Selectivity index
GRL-02031	0.028 ± 0.003	>100	>3,600
SQV	0.014 ± 0.005	9.9 ± 3.6	710
APV	0.033 ± 0.012	>100	>3,000
IDV	0.044 ± 0.007	69.8 ± 3.1	1,600
RTV	0.038 ± 0.004	21.3 ± 0.9	560
NFV	0.023 ± 0.006	ND	ND
LPV	0.032 ± 0.007	ND	ND

[a] MT-2 cells (2×10^4/ml) were exposed to 100 $TCID_{50}$s of HIV-1_{LAI} and were cultured in the presence of various concentrations of PIs, and the EC_{50}s were determined by using the MTT assay on day 7 of culture. All assays were conducted in duplicate. The data shown represent mean values (±1 standard deviation) derived from the results of three independent experiments. ND, not determined. Selectivity index, CC_{50}/EC_{50}.

sequences of the plasmids confirmed that each clone had the desired mutations but no unintended mutations. Each recombinant plasmid was transfected into 293T cells with Lipofectoamine 2000 transfection reagent (Invitrogen, Carlsbad, CA), and the infectious virions thus generated were harvested for 48 h after transfection and stored at −80°C until use.

Structural analysis of GRL-02031 interactions with wild-type HIV-1 protease. The interactions of GRL-02031 with wild-type HIV-1 protease were examined by computational structural modeling and molecular docking on the basis of the published crystallographic data for protease complexed with PIs. Besides accounting for the conformational flexibility of the inhibitor, the polarization induced in the inhibitor by the protease was taken into consideration by employing polarizable quantum charges in the docking computations. The use of polarizable quantum charges has recently been shown to substantially improve the prediction of protein-ligand complex structures (4). The quantum mechanical polarized ligand docking protocol provided with the Glide (version 4.5), QSite (version 4.5), Jaguar (version 7.0), and Maestro (version 8.5) software (Schrödinger, LLC, New York, NY) was used as described below. The crystal structures 2FDE (protease-brecanavir complex) and 2IEN (protease-DRV complex) were used as templates in separate docking calculations to determine the binding mode of GRL-02031 with wild-type protease. The crystal coordinates were obtained from the Protein Data Bank (http://www.rcsb.org/). Hydrogens were optimized by placing constraints on the heavy atoms. The crystal water that mediates the interaction between PIs and the protease flap was retained, and all other crystal waters were deleted. Close interaction in the protease was annealed, and the docking grid was set up. Polarizable ligand charges were determined at the B3LYP/6-31G* level. The extraprecision mode of the Glide program (12, 13), which has a higher penalty for unphysical interactions, was used.

RESULTS

In vitro activity of GRL-02031 against laboratory and primary HIV strains and cytotoxicity of GRL-02031. We designed and synthesized ~80 different novel nonpeptidyl PIs containing a Cp-THF moiety and examined them for their anti-HIV activities and cytotoxicities in vitro. Among them, we found that GRL-02031 (Fig. 1) was the most potent against a laboratory HIV-1 strain, HIV-1_{LAI}, and had a favorable cytotoxicity profile, as examined with target MT-2 cells. As shown in Table 1, GRL-02031 showed an anti-HIV-1 activity profile comparable to that of most of the Food and Drug Administration (FDA)-approved PIs examined in the present study, although its toxicity profile was apparently more favorable, with a 50% cytotoxic concentration (CC_{50}) of >100 μM and a selectivity index (CC_{50}/EC_{50}) of >3,600.

GRL-02031 was further tested against two R5 laboratory HIV-1 strains (HIV-$1_{Ba\text{-}L}$ and HIV-1_{JRFL}), three different subtypes of primary HIV-1 strains (HIV-$1_{92UG037}$ [subtype A], HIV-$1_{97ZA003}$ [subtype C], and HIV-$1_{92TH019}$ [subtype E]), and two HIV-2 strains (HIV-2_{ROD} and HIV-2_{EHO}). GRL-02031 was found to be potent against all these HIV-1 strains and had EC_{50}s that ranged from 0.015 to 0.038 μM, as tested by the use of target PHA-PBMs, while GRL-02031 was moderately active against two HIV-2 strains (EC_{50}, ~0.60 μM), as tested by the use of MT-2 cells (data not shown).

GRL-02031 exerts potent activity against a wide spectrum of primary HIV-1 variants resistant to multiple PIs. We next examined the activity of GRL-02031 against a variety of primary HIV-1 strains which were isolated from those with AIDS who had failed a number of anti-HIV therapeutic regimens after they had received 9 to 11 anti-HIV-1 drugs over the previous 32 to 83 months and who proved to be highly resistant to multiple PIs (47, 48). These primary strains contained 9 to 14 amino acid substitutions in the protease-encoding region of the HIV-1 genome which have been reported to be associated with HIV-1 resistance to various PIs (RTV, IDV, NFV, SQV, APV, and LPV) (8). The substitutions identified included Leu-10 → Ile (L10I; seven of seven isolates), M46I/L (six of seven isolates), I54V (five of seven isolates), L63P (seven of seven isolates), A71V/T (six of seven isolates), V82A or V82T (seven of seven isolates), and L90M (five of seven isolates) (see footnote *a* of Table 2).

All drugs examined showed potent activity against two reference wild-type primary strains (X4 HIV-$1_{ERS104pre}$ [45] and R5 HIV-1_{MOKW} [30]), with the EC_{50}s ranging 0.004 to 0.036 μM (Table 2). However, all the primary strains examined were highly resistant to AZT, with the EC_{50}s being from 24- to >200-fold greater than the EC_{50} against HIV-$1_{ERS104pre}$. It was noted that SQV and LPV were still active against one or two of the seven strains and had EC_{50}s that differed 3- to 4-fold from those for HIV-$1_{ERS104pre}$; however, all the other FDA-approved PIs examined in this study except DRV failed to exert activity and had EC_{50}s 6- to >63-fold greater than the EC_{50} for HIV-$1_{ERS104pre}$. In contrast, GRL-02031, like DRV, potently blocked all seven primary strains and had EC_{50}s that ranged from 0.014 to 0.043 μM. It should be noted that the change in the EC_{50} of GRL-02031 for all seven multi-PI-resistant isolates tested was less than twofold compared with the EC_{50} for a wild-type primary strain, HIV-$1_{ERS104pre}$.

Selection of HIV-1_{NL4-3} with GRL-02031. We then attempted to select a laboratory X4 HIV-1 strain (HIV-1_{NL4-3}) by propagating it in MT-4 cells in the presence of increasing concentrations of APV, IDV, or GRL-02031, as described previously (47). The virus was initially exposed to 0.03 μM APV, 0.02 μM IDV, or 0.02 μM GRL-02031. At passages 21 and 27, HIV-1_{NL4-3} was capable of propagating in the presence of 167- and 250-fold greater concentrations of APV and IDV, respectively. At passage 26, HIV-1_{NL4-3} was capable of propagating in the presence of a 250-fold greater concentration of IDV; however, 37 passages were required until the virus became similarly resistant to GRL-02031 and capable of propagating in the presence of 5 μM (Fig. 2).

We also determined the nucleic acid sequences of the protease-encoding region of the proviral DNA isolated from the cells exposed to GRL-02031 at passages 5, 15, 22, 30, and 37 (Fig. 3). At passage 5, no significant amino acid substitutions were identified; however, by passage 15, the virus had acquired the L10F substitution, which has been reported to be associated with PI resistance (6, 32). By passage 22, all eight clones of the virus examined had additionally acquired a flap muta-

TABLE 2. Antiviral activity of GRL-02031 against clinical HIV-1 isolates in PHA-PBMs[a]

Virus	Phenotype	EC_{50} (μM)							
		AZT	SQV	APV	IDV	NFV	RTV	LPV	DRV	GRL-02031
HIV-$1_{ERS104pre}$ (wild type)	X4	0.005 ± 0.002	0.009 ± 0.005	0.025 ± 0.007	0.021 ± 0.008	0.016 ± 0.004	0.036 ± 0.008	0.032 ± 0.002	0.0035 ± 0.0003	0.027 ± 0.002
HIV-1_{MOKW} (wild type)	R5	0.016 ± 0.011	0.004 ± 0.002	0.015 ± 0.004	0.019 ± 0.005	0.023 ± 0.008	0.036 ± 0.008	0.029 ± 0.0005	0.003 ± 0.0005	0.026 ± 0.007
HIV-1_{TAM}(MDR)	X4	0.89 ± 0.11 (178)	0.27 ± 0.08 (30)	0.35 ± 0.11 (14)	>1 (>48)	>1 (>63)	>1 (>30)	0.23 ± 0.18 (7)	0.004 ± 0.001 (1)	0.026 ± 0.004 (1)
HIV-1_{MM}(MDR)	R5	0.45 ± 0.08 (90)	0.27 ± 0.06 (30)	0.40 ± 0.10 (16)	>1 (>48)	>1 (>63)	>1 (>30)	0.62 ± 0.28 (19)	0.017 ± 0.008 (5)	0.041 ± 0.004 (2)
HIV-1_{ISL} (MDR)	R5	0.18 ± 0.11 (36)	0.32 ± 0.13 (36)	0.66 ± 0.17 (26)	>1 (>48)	>1 (>63)	>1 (>30)	0.74 ± 0.32 (23)	0.026 ± 0.005 (7)	0.043 ± 0.003 (2)
HIV-1_A(MDR)	X4	0.12 ± 0.11 (24)	0.10 ± 0.07 (11)	0.16 ± 0.08 (6)	>1 (>48)	0.33 ± 0.07 (21)	>1 (>30)	0.32 ± 0.003 (10)	0.003 ± 0.0003 (1)	0.014 ± 0.007 (1)
HIV-1_B(MDR)	X4	>1 (>200)	0.30 ± 0.02 (33)	0.31 ± 0.04 (12)	>1 (>48)	>1 (>63)	>1 (>30)	0.25 ± 0.007 (8)	0.026 ± 0.017 (7)	0.029 ± 0.007 (1)
HIV-1_C(MDR)	X4	0.28 ± 0.20 (56)	0.033 ± 0.010 (4)	0.22 ± 0.13 (9)	>1 (>48)	0.36 ± 0.12 (23)	>1 (>30)	0.46 ± 0.24 (14)	0.007 ± 0.005 (2)	0.027 ± 0.009 (1)
HIV-1_G(MDR)	X4	0.60 ± 0.56 (120)	0.027 ± 0.006 (3)	0.23 ± 0.13 (9)	0.34 ± 0.07 (16)	0.23 ± 0.11 (14)	>1 (>30)	0.13 ± 0.04 (4)	0.01	004 (2)	0.028 ± 0.001 (1)

[a] The amino acid substitutions identified in the protease-encoding region of HIV-$1_{ERS104pre}$, HIV-1_{TAM}, HIV-1_{MM}, HIV-1_{ISL}, HIV-1_A, HIV-1_B, HIV-1_C, and HIV-1_G compared to the Los Alamos National Laboratory database include L63P, L10I/K14R/R41K/M46L/I54V/L63P/A71V/V82A/L90M/I93L; L10I/K43T/M46L/I54V/L63P/A71V/V82A/L90M/Q92K, L10I/L24I/L33F/E35D/M36I/N37S/M46L/I54V/R57K/I62V/L63P/A71V/G73S/V82A, L10I/I15V/E35D/N37E/K45R/I54V/L63P/A71V/V82T/L90M/I93L/C95F, L10I/K14R/L33I/M36I/M46I/F53L/K55R/I62V/L63P/A71V/G73S/V82A/L90M/I93L, L10I/I15V/K20R/L24I/M36I/M46L/I54V/I62V/L63P/K70Q/V82A/L89M, and L10I/V11I/T12E/I15V/L19I/R41K/M46L/L63P/A71V/V82A/L90M, respectively. HIV-1_{MOKW} was confirmed to lack known drug resistance-associated amino acid substitutions. The EC_{50}s were determined by employing PHA-PBMs as target cells and the inhibition of p24 Gag protein production as the endpoint. All values were determined in triplicate, and those shown were derived from the results of three independent experiments. Numbers in parentheses represent the fold changes in the EC_{50} for each isolate compared to the EC_{50} for HIV-$1_{ERS104pre}$. MDR, multidrug resistant.

FIG. 2. In vitro selection of HIV-1 variants resistant to GRL-02031. HIV-1_{NL4-3} was passaged in the presence of increasing concentrations of APV (open circles), IDV (solid circles), or GRL-02031 (open triangles) in MT-4 cells. The selection was carried out in a cell-free manner for a total of 21 to 37 passages with drug concentrations escalating from 0.02 to 5 μM. The nucleotide sequences of the proviral DNAs were determined by using cell lysates of HIV-1-infected MT-4 cells at the termination of each indicated passage.

tion (I47V) and the primary substitution (V82I). By passage 30, in addition to L10F, I47V, and V82I, the virus had acquired L33F, M46I, and I85V. By passage 37, the virus had gained I84V and another Q58E substitution, an unusual mutation not associated with resistance to other HIV PIs. Genetic characterization of the protease-encoding gene of the HIV-1 variants selected with APV and IDV revealed that those variants had acquired previously reported mutations, such as L10F, V32I, M46I, and I84V in APV-selected HIV-1 (HIV-$1_{APV}{}^r$) and L10F, V32I, K43T, M46I, L63P, G73C, and V82A in HIV-$1_{IDV}{}^r$.

Amino acid substitutions in Gag protein of HIV-1 exposed to GRL-02031. We also determined the amino acid sequences of the Gag proteins of HIV-1_{NL4-3} exposed to GRL-02031. By passage 15, an unusual amino acid substitution, L363M, located at the p24-p2 cleavage site, had emerged. By passage 22, the virus had acquired another amino acid substitution, I437T, located close to the p7-p1 cleavage site. By passage 30 and beyond, G62R (within p17) and R409K (within p7) were seen in addition to L363M and I437T (data not shown).

Anti-HIV-1 profile of a GRL-02031-resistant HIV-1 variant. We then examined the anti-HIV-1 profile of a GRL-02031-resistant HIV-1 variant. In this experiment, we employed eight HIV-1 variants which were selected in the presence of up to 1 or 5 μM of each of seven FDA-approved PIs and GRL-02031. Each of these eight variants contained a variety of previously known PI resistance-associated amino acid substitutions (see footnote *a* of Table 3). As shown in Table 3, when each HIV-1 variant was examined in target MT-4 cells, each HIV-1 variant except the variant selected with 1 μM LPV in vitro (HIV-$1_{LPV\text{-}1\ \mu M}$) and the variant selected with 1 μM ATV in vitro (HIV-$1_{ATV\text{-}1\ \mu M}$), proved to be highly resistant to the PI with which the virus was selected, with EC_{50}s exceeding 1 μM. However, GRL-02031 was potent against all the PI-resistant variants, although the compound was relatively less potent against the variant selected with 5 μM SQV in vitro (HIV-

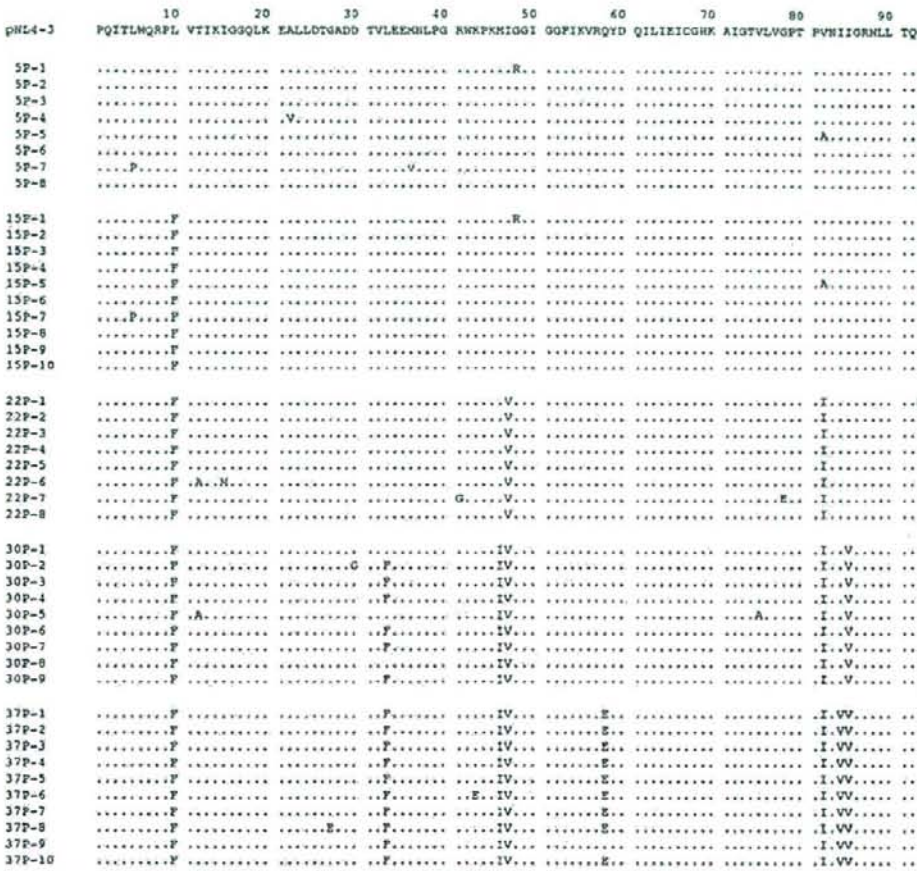

FIG. 3. Sequence analysis of the protease-encoding region of HIV passaged in the presence of GRL-02031. The amino acid sequences of the proteases deduced from the nucleotide sequences of the protease-encoding region of HIV clones determined at five different passages are illustrated. The identity of each amino acid with that from pNL4-3 (top row) at each individual amino acid position is indicated by a dot.

$1_{SQV\text{-}5\ \mu M}$) (a sixfold increase in the EC_{50} of SQV compared with that of GRL-02031).

When the virus was selected with up to 5 μM GRL-02031 (HIV-$1_{GRL\text{-}02031\text{-}5\ \mu M}$) was examined in MT-4 cells, the EC_{50} of GRL-02031 turned out to be >1 μM although HIV-$1_{GRL\text{-}02031\text{-}5\ \mu M}$ remained susceptible to other PIs, in particular, SQV, IDV, and NFV. The HIV-$1_{LPV\text{-}1\ \mu M}$ variant was substantially resistant to APV, IDV, NFV, RTV, LPV, and ATV; however, this variant was highly susceptible to GRL-02031 and had an EC_{50} of 0.038 μM (Table 3). HIV-$1_{ATV\text{-}1\ \mu M}$ variant was also substantially resistant to IDV, NFV, and ATV; however, this variant was susceptible to LPV and GRL-02031. Of note, LPV, which has currently been widely used as a first-line therapeutic among HAART regimens, was not active against three HIV-1 variants (HIV-$1_{SQV\text{-}5\ \mu M}$, a variant selected with 5 μM IDV [HIV-$1_{IDV\text{-}5\ \mu M}$], and a variant selected with 5 μM NFV [HIV-$1_{NFV\text{-}5\ \mu M}$]), with the differences in the EC_{50}s being more than 16-fold compared to the value for wild-type strain HIV-$1_{NL4\text{-}3}$. This anti-HIV-1 profile of LPV greatly contrasted with that of GRL-02031. GRL-02031 was highly potent against all the variants examined except HIV-$1_{SQV\text{-}5\ \mu M}$ (sixfold change in the EC_{50} compared to that for HIV-$1_{NL4\text{-}3}$). It is also noteworthy that SQV, IDV, and NFV remained potent against HIV-$1_{GRL\text{-}02031\text{-}5\ \mu M}$, suggesting that the combination of GRL-02031 and SQV, IDV, or NFV could exert complementarily augmented activity against multi-PI-resistant HIV-1 variants.

Sensitivities of infectious molecular HIV-1 clones carrying various amino acid substitutions to GRL-02031. Finally, we attempted to determine the profile of the activity of GRL-02031 against a variety of HIV-$1_{NL4\text{-}3}$-based molecular infectious clones containing a single primary mutation previously reported or a combination of such mutations (Table 4) (21, 31, 40–42). Interestingly, no significant changes in EC_{50}s were observed when HIV-1 clones containing only one of the amino acid substitutions (L10F, L33F, M46I, I47V, Q58E, V82I,

TABLE 3. Antiviral activities of GRL-02031 against laboratory PI-resistant HIV-1 variants[a]

Virus	EC_{50} (μM)							
	SQV	APV	IDV	NFV	RTV	LPV	ATV	GRL-02031
HIV-1_{NL4-3}	0.008 ± 0.004	0.028 ± 0.009	0.014 ± 0.004	0.018 ± 0.009	0.021 ± 0.009	0.018 ± 0.001	0.0043 ± 0.0004	0.023 ± 0.008
HIV-$1_{SQV-5\ \mu M}$	>1 (>125)	0.21 ± 0.09 (8)	>1 (>71)	0.32 ± 0.04 (18)	>1 (>48)	0.70 ± 0.22 (39)	0.32 ± 0.02 (74)	0.14 ± 0.06 (6)
HIV-$1_{APV-5\ \mu M}$	0.016 ± 0.010 (2)	>1 (>36)	0.22 ± 0.15 (16)	0.17 ± 0.10 (10)	>1 (>48)	0.14 ± 0.05 (8)	0.0032 ± 0.012 (1)	0.037 ± 0.004 (2)
HIV-$1_{IDV-5\ \mu M}$	0.022 ± 0.009 (3)	0.26 ± 0.14 (9)	>1 (>71)	0.65 ± 0.16 (36)	>1 (>48)	>1 (>56)	0.063 ± 0.022 (15)	0.047 ± 0.002 (2)
HIV-$1_{NFV-5\ \mu M}$	0.028 ± 0.009 (4)	0.078 ± 0.026 (3)	0.27 ± 0.06 (19)	>1 (>56)	0.08 ± 0.05 (4)	0.29 ± 0.03 (16)	0.024 ± 0.005 (6)	0.036 ± 0.002 (2)
HIV-$1_{RTV-5\ \mu M}$	0.010 ± 0.008 (1)	0.43 ± 0.27 (15)	0.30 ± 0.07 (21)	0.24 ± 0.10 (13)	>1 (>48)	0.11 ± 0.08 (6)	0.021 ± 0.007 (5)	0.077 ± 0.031 (3)
HIV-$1_{LPV-1\ \mu M}$	0.033 ± 0.003 (4)	0.32 ± 0.02 (11)	>1 (>71)	0.51 ± 0.06 (28)	>1 (>48)	0.30 ± 0.04 (17)	0.041 ± 0.002 (10)	0.038 ± 0.004 (2)
HIV-$1_{ATV-1\ \mu M}$	0.034 ± 0.006 (4)	0.18 ± 0.06 (6)	0.33 ± 0.10 (24)	0.21 ± 0.03 (12)	0.14 ± 0.02 (7)	0.025 ± 0.011 (1)	0.31 ± 0.05 (72)	0.033 ± 0.002 (1)
HIV-$1_{GRL-02031-5\ \mu M}$	0.008 ± 0.001 (1)	0.21 ± 0.02 (8)	0.044 ± 0.015 (3)	0.011 ± 0.004 (1)	0.26 ± 0.10 (12)	0.14 ± 0.09 (8)	0.036 ± 0.005 (8)	>1 (>43)

[a] The amino acid substitutions identified in the protease-encoding region of HIV-$1_{SQV-5\ \mu M}$, HIV-$1_{APV-5\ \mu M}$, HIV-$1_{IDV-5\ \mu M}$, HIV-$1_{NFV-5\ \mu M}$, HIV-$1_{RTV-5\ \mu M}$, HIV-$1_{LPV-1\ \mu M}$, HIV-$1_{ATV-1\ \mu M}$, and HIV-$1_{GRL-02031-5\ \mu M}$ compared to the consensus B sequence cited from the Los Alamos National Laboratory database include L10I/G48V/I54V/L90M, L10F/V32I/M46I/I54M/A71V/I84V, L10F/L24I/M46I/L63P/A71V/G73S/V82T, L10F/D30N/K45I/A71V/T74S, M46I/V82F/I84V, L10F/M46I/I54V/V82A, I23I/K43I/M46I/I50L/G51A/A71V, and L10F/L33F/M46I/I47V/Q58E/V82I/I84V/I85V, respectively. MT-4 cells (1×10^5) were exposed to each HIV-1 isolate (100 $TCID_{50}$s), and the inhibition of p24 Gag protein production by the drug was used as the endpoint. The numbers in parentheses represent the fold changes in the EC_{50}s for each isolate compared to the EC_{50} for HIV-1_{NL4-3}. The data shown are mean values (±1 standard deviation) derived from the results of three independent experiments conducted in triplicate.

I84V, or I85V) which emerged in the selection process in the present work (Fig. 3) were tested with GRL-02031. We tested each of these one-mutation-containing infectious clones against a selected PI, and again, no significant changes in EC_{50}s were seen (Table 4).

It was noted that increases in the EC_{50}s of GRL-02031 were seen only when more than two amino acid substitutions were introduced into HIV-1_{NL4-3}. A substantial reduction in susceptibility (differences in EC_{50}s of more than threefold) was seen when the virus had two mutations (M46I/I47V or I84V/I85V). Further increases in the EC_{50}s were seen when four substitutions (L10F/I47V/V82I/I85V) or five substitutions (L10F/M46I/I47V/V82I/I85V) were introduced. Moreover, we generated molecular clones containing a primary mutation with which HIV-1 is known to acquire substantial resistance to a PI(s) (such as D30N, G48V, I50V, and L90M) and determined the EC_{50}s of GRL-02031 (Table 4). We found that GRL-02031 was potent against all such molecular clones with a primary mutation, with the differences in the EC_{50}s being 0.7- to 1.7-fold in comparison with the EC_{50} for HIV-1_{NL4-3}, although HIV-1_{D30N} and HIV-1_{G48V} showed moderate to substantial levels of resistance to NFV (5.6-fold change) and SQV (5.1-fold change) (Table 4). These data suggest that HIV-1 can acquire substantial resistance to GRL-02031 only when it gains multiple mutations in the protease, a potentially advantageous property of GRL-02031.

Structural analysis of GRL-02031 interactions with wild-type protease. Finally, we conducted molecular and structural analyses of the interactions of GRL-02031 with protease (Fig. 4). By refined structural modeling based on the previously published crystal structures 2FDE (protease-brecanavir complex) and 2IEN (protease-DRV complex), we found that the oxygen atom of Cp-THF has a hydrogen bond interaction with Asp29 in the S-2 pocket of the protease. The hydrogen bond interactions of GRL-02031 with Asp25 and Gly27, which have been observed for various PIs, were also predicted to be present. In addition, GRL-02031 has hydrogen bond interactions mediated through a water molecule with flap residues Ile50 and Ile50′. Of note, GRL-02031 has an *R* configuration at the pyrrolidone stereocenter. Interestingly, the structural models demonstrated that for the *R*-stereochemical configuration, two distinct binding modes of GRL-02031 were found in the S-2′ pocket. The 2-pyrrolidone group and the methoxybenzene moiety can orient toward Asp29′ and Asp30′ for configuration 1 and configuration 2, respectively (Fig. 4A and B). In configuration 1, the 2-pyrrolidone oxygen has hydrogen bond interactions with Asp29′ in the S-2′ pocket. In configuration 2, the methoxybenzene orients toward the S-2′ pocket and forms tight hydrogen bonds with Asp30′. The interactions of PIs (48) with Asp29′ and/or Asp30′ have been reported to be mediated by water molecules. It is likely that the presence of water molecules may influence the relative abundance of configurations 1 and 2. The alternate bimodal binding feature observed in this molecular analysis should provide advantages to the PI in maintaining its antiviral potency when the HIV-1 protease either has a polymorphism or develops amino acid substitutions under drug pressure.

We also examined the lipophilic potential of the computationally defined cavity for the binding of GRL-02031 within the HIV protease (Fig. 4C). It was revealed that GRL-02031 fits

TABLE 4. Sensitivities of infectious molecular HIV clones carrying various amino acid substitutions to GRL-02031[a]

Recombinant HIV-1 clone	EC_{50} (μM) of GRL-02031	Fold change in EC_{50}	Fold change in EC_{50} compared with that of other PIs	Fold change in EC_{50} of other PIs reported previously (reference)
pNL4-3 (wild-type)	0.023 ± 0.008	1.0		
L10F	0.037 ± 0.001	1.6	1.4 (APV)	1.5 (IDV) (42)
L33F	0.028 ± 0.005	1.2	1.0 (RTV)	1.4 (APV) (31)
M46I	0.028 ± 0.009	1.2	1.2 (RTV)	1.0 (APV) (40)
I47V	0.037 ± 0.006	1.6	1.2 (APV)	2.2 (APV) (31)
Q58E	0.033 ± 0.007	1.4	1.0 (APV)	Not previously reported
V82I	0.035 ± 0.001	1.5	1.5 (RTV)	1.9 (APV) (31)
I84V	0.030 ± 0.0001	1.3	2.2 (IDV)	10.6 (IDV) (41)
I85V	0.024 ± 0.011	1.0	2.1 (RTV)	Not previously reported
M46I/I47V	0.073 ± 0.009	3.2	1.3 (APV)	1.0 (APV) (40)
V82I/I85V	0.035 ± 0.002	1.5	1.6 (RTV)	Not previously reported
I84V/I85V	0.097 ± 0.010	4.2	14.8 (RTV)	Not previously reported
L10F/I47V/V82I/I85V	0.43 ± 0.06	18.7	1.9 (RTV)	Not previously reported
L10F/M46I/I47V/V82I/I85V	>1	>43	10.0 (APV)	Not previously reported
D30N	0.020 ± 0.009	0.9	5.6 (NFV)	6.0 (NFV) (41)
G48V	0.040 ± 0.0008	1.7	5.1 (SQV)	7.0 (SQV) (21)
I50V	0.015 ± 0.008	0.7	1.2 (APV)	3.5 (APV) (31)
L90M	0.032 ± 0.001	1.4	1.0 (SQV)	3.0 (SQV) (21)

[a] MT-4 cells (1×10^4/ml) were exposed to 100 $TCID_{50}$s of each infectious molecular HIV clone, and the inhibition of p24 Gag protein production by the drug was used as the endpoint on day 7 in culture. The fold change represents the ratio of the EC_{50} for each mutant clone to the EC_{50} for wild-type HIV-1_{NL4-3}. All assays were performed in triplicate, and the values shown are mean values (±1 standard deviation) derived from the results of three independent experiments.

tightly in the binding cavity and has favorable polar and nonpolar interactions with the active-site residues of the HIV-1 protease. The van der Waals surfaces of Ile47 and Ile47′ and of Ile84′ demonstrate that they form tight nonpolar interactions with GRL-02031. Our antiviral data showing that the I47V substitution is associated with HIV-1 resistance to GRL-02031 (Tables 3 and 4) are in agreement with this structural finding, in that the substitution should reduce GRL-02031's interaction with protease and helps develop HIV-1 resistance to the inhibitor.

DISCUSSION

In the present work, we demonstrated that GRL-02031 suppresses the replication of a wide spectrum of HIV-1 isolates and is potent against a variety of HIV-1 variants highly resistant to multiple PIs, with the differences in the EC_{50}s being less than twofold in comparison with the EC_{50} for wild-type strain HIV-$1_{ERS104pre}$ (Table 2). Additionally, when HIV-1_{NL4-3} was propagated in the presence of increasing concentrations of IDV, APV, or GRL-02031, the time of emergence of HIV-1 variants highly resistant to GRL-02031 was substantially delayed compared to that of IDV- or APV-resistant HIV-1 variants (Fig. 2). Indeed, 21, 27, and 37 passages were required for HIV-1 to acquire the ability to propagate in the presence of APV, IDV, and GRL-02031 at 5 μM, respectively. In this regard, when we generated a variety of PI-resistant HIV-1 variants by propagating laboratory strain HIV-1_{NL4-3} in the presence of increasing concentrations of a PI in MT-4 cells using the same procedure as that used in the present study, it required 27, 23, 22, 21, and 14 passages for the virus to propagate in the presence of 5 μM of SQV, APV, IDV, NFV, and RTV, respectively (26). However, it should be noted that the population size of HIV-1 in a culture is relatively small and that the viral acquisition of mutations can be affected by stochastic phenomena. For example, mutations take place at random and the rates of mutations in the HIV-1 genome may not be reproducible, although certain mutations that severely compromise viral replication would not remain in culture.

During the selection of HIV-1_{NL4-3} with GRL-02031, the L10F substitution, one of the secondary substitutions, first appeared. The L10F mutation occurs distal to the active site of the enzyme and is thought to act in concert with active-site mutations and compensate for a possible functional deficit caused by the latter (6, 32). Mutations at Leu-10 reportedly occur in 5 to 10% of HIV-1 isolates recovered from untreated HIV-1-infected individuals but increase in prevalence by 60 to 80% in heavily treated patients (19, 22). However, the virological and structural significance of the L10F substitution in HIV-1 resistance to GRL-02031 is presently unknown.

By passage 37, two active-site mutations (V82I and I84V) emerged. These V82 and I84 residues represent active-site residues whose side chains are involved in the formation of the protease substrate cleft and that make direct contact with certain PIs (48), and the V82I substitution has been shown to be effective in conferring resistance when it is combined with a second active-site mutation, such as V32I (23). Another active-site mutation (I85V) and two flap mutations (M46I and I47V) also emerged by passage 30. Both Met46 and Ile47 are located in the flap region of the enzyme; the I47V substitution is reported to be associated with viral resistance to APV and JE-2147 (40, 48). The lipophilic potential of the computationally defined cavity for the binding of GRL-02031 within the HIV protease seems to be related to a finding that the van der Waals surfaces of Ile47 and Ile47′ and of Ile84′ form tight nonpolar interactions with GRL-02031 (Fig. 4C). Our antiviral data showing that the I47V substitution is associated with HIV-1 resistance to GRL-02031 (Table 3) are in agreement with this structural finding. However, it is also of note that HIV-1 acquires substantial resistance to GRL-02031 when the virus gains multiple mutations in the protease (Table 4), as

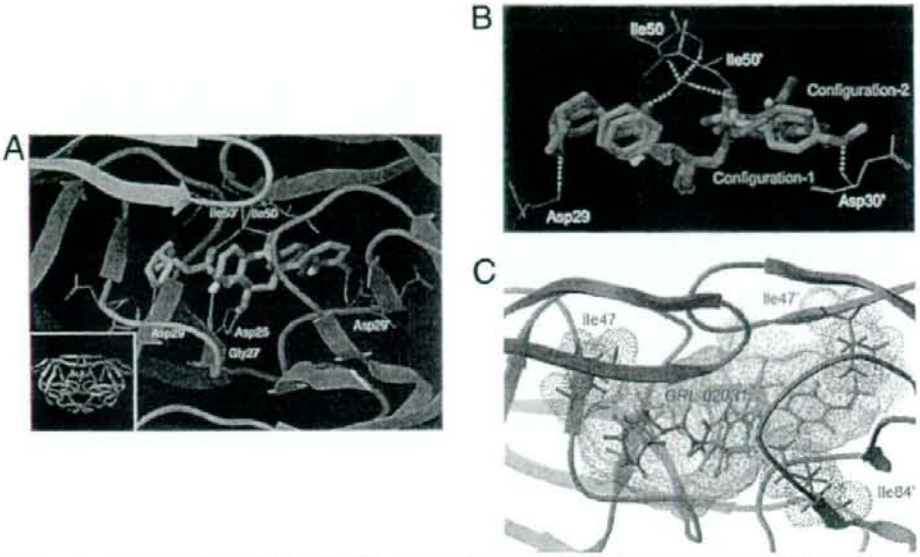

FIG. 4. Molecular interactions of GRL-02031 with HIV-1 protease. (A) A model of the interaction of GRL-02031 with HIV protease. The bird's-eye view of the docked pose (inset) is presented along with a blown-up figure highlighting the important hydrogen bond interactions. The inhibitor is predicted to have hydrogen bond interactions with Asp25, Gly27, Asp29, Ile50, Asp29′, and Ile50′. Note that the pyrrolidone oxygen (red stick) interacts with the S-2′ subpocket and forms a hydrogen bond interaction with Asp29′. (B) Superimposed binding configurations of GRL-02031 with the HIV-1 protease. The carbons are shown in gray in configuration 1 and in green in configuration 2. Selected hydrogen bond interactions of configuration 2 are shown. In configuration 2, the methoxybenzene interacts with the S-2′ site and forms a hydrogen bond interaction with Asp30′. The interaction of the P-2 ligand Cp-THF is the same in both configurations. (C) The binding cavity of HIV protease with lipophilic potential is shown. GRL-02031 fits tightly in the binding cavity and has favorable polar and nonpolar interactions with the active-site residues of the HIV-1 protease. The van der Waals surfaces of Ile47 and Ile47′ (both in magenta) and of Ile84′ (in purple) demonstrate that they form tight nonpolar interactions with GRL-02031. The protease residues are shown in stick representation. The following atoms are indicated by designated colors: C, gray; O, red; N, blue; S, yellow; H, cyan. Both protease chains are shown in green. The figure was generated with the MOLCAD program (Sybyl, version 8.0; Tripos, L.P, St. Louis, MO).

seen in the case of DRV (9). This resistance profile (i.e., the requirement of multiple mutations) of GRL-02031 may also confer certain advantage in the resistance profile of GRL-02031.

Two mutations at conserved residues, L33F and Q58E, also emerged by passage 37 and were present in 10 and 9 of 10 clones, respectively. L33F has primarily been reported in patients treated with RTV or APV (37). The L33F substitution alone did not change the susceptibility of HIV-1 to GRL-02031 (Table 4), although it has recently gained attention because of its association with resistance to the FDA-approved PI, tipranavir (33).

In the HIV-1 variants selected with GRL-02031, four amino acid substitutions in the Gag proteins (G62R, R409K, L363M, and I437T) were seen by passage 37. R409K within the p7 Gag seems to be associated with viral resistance to APV (14), although the significance of G62R within p17 is as yet unknown. The p7-p1 cleavage-site mutation I437T has been reported to be associated with ATV resistance (17). It is of note that by passage 15, an unusual amino acid substitution, L363M, emerged; this substitution has not previously been reported in relation to PI resistance. This L363M is located at the p24-p2 cleavage site, which represents the C terminus of the capsid (CA) p24 protein that is highly conserved and that is involved in virion assembly. The deletion of this cluster or the introduction of mutations such as L363A is known to cause significant impairment of particle formation and infectivity (34). It is noteworthy that L363M appears in HIV-1 variants resistant to a maturation inhibitor, PA-457 [3-*O*-(3′,3′-dimethylsuccinyl) betulinic acid], which binds to the CA-p2 cleavage site or its proximity, blocks the cleavage by protease during virion maturation, and exerts activity against HIV-1 (27, 44, 49).

It was noted that GRL-02031 and SQV remained active against most of the PI-selected HIV-1 variants and that SQV, IDV, and NFV remained potent against HIV-$1_{GRL\text{-}02031\text{-}5\ \mu M}$ (Table 3), suggesting that the combination of GRL-02031, SQV, IDV, and NFV can exert complementarily augmented activity against multi-PI-resistant HIV-1 variants. Such a difference in the resistance profile of GRL-02031 when it is used with SQV and NFV may be due to the differences in binding and antiviral potency associated with the D30N and G48V mutations (Table 4).

In an attempt to explain why GRL-02031 can exert potent activity against a wide spectrum of HIV-1 variants resistant to multiple PIs, we performed structural modeling and molecular docking of the interactions of GRL-02031 with protease (Fig. 4). Interestingly, our structural modeling analysis demonstrated that there are two distinct binding modes of GRL-

02031 in the S-2′ pocket of the protease. Either the 2-pyrrolidone group or the methoxybenzene moiety can orient toward Asp29′ and Asp30′ (configuration 1 and configuration 2, respectively) (Fig. 4B). It is presumed that such alternate binding modes provide distinct advantages to GRL-02031 in maintaining its antiviral activity against a wide spectrum of HIV-1 variants resistant to other currently available PIs. The alternate binding modes could explain the reason why the development of resistance to GRL-02031 is substantially delayed compared to the time to the development of resistance to APV or IDV (Fig. 2). In addition, the models of GRL-02031 indicated that it is capable of forming hydrogen bond interactions with the backbone atoms of Asp29, Asp29′, and/or Asp30′. Such backbone interactions have been shown to be important in maintaining potency not only against wild-type protease but also against drug-resistant mutant proteases (1, 15, 16, 36). This may also explain why GRL-02031 maintains its potency against a wide variety of drug-resistant mutant proteases.

It is of note that the difference seen with GRL-02031 (one- to twofold) seems substantially less than that seen with DRV (one- to sevenfold) (Table 2). Although this difference may not be translated into an actual difference in the clinical setting, it is worth noting that GRL-02031 may have certain advantages in its activity against highly drug-resistant HIV-1 variants. Considering that the acquisition of multiple amino acid substitutions is required for the emergence of HIV-1 resistance to GRL-02031, the profile of HIV-1 resistance to GRL-02031, which is apparently different from the profiles for the other PIs, might result in an advantage for GRL-02031, although further evaluations, including testing of the compound in the clinical setting, are required.

Taken together, GRL-02031 exerts potent activity against a wide spectrum of laboratory and clinical wild-type and multidrug-resistant HIV-1 strains without significant cytotoxicity in vitro and substantially delays the emergence of HIV-1 variants resistant to GRL-02031. These data warrant further consideration of GRL-02031 as a candidate as a novel PI for the treatment of AIDS.

ACKNOWLEDGMENTS

We thank Shintaro Matsumi, Toshikazu Miyakawa, and Manabu Aoki for helpful discussion.

This work was supported in part by the Intramural Research Program of the Center for Cancer Research, National Cancer Institute, National Institutes of Health (to D.D., H.N., and H.M.); a grant from the National Institutes of Health (grant GM 53386 to A.K.G.); a grant from a Research for the Future Program of the Japan Society for the Promotion of Science (grant JSPS-RFTF 97L00705 to H.M.); a Grant-in-Aid for Scientific Research (grant for priority areas to H.M.) from the Ministry of Education, Culture, Sports, Science, and Technology (Monbu-Kagakusho) of Japan; and a Grant for Promotion of AIDS Research from the Ministry of Health, Labor and Welfare (Kosei-Rodosho) of Japan (to H.M.).

This work utilized the computational resources of the Biowulf cluster at the NIH.

REFERENCES

1. **Amano, M., Y. Koh, D. Das, J. Li, S. Leschenko, Y. F. Wang, P. I. Boross, I. T. Weber, A. K. Ghosh, and H. Mitsuya.** 2007. A novel bis-tetrahydrofuranylurethane-containing nonpeptidic protease inhibitor (PI), GRL-98065, is potent against multiple-PI-resistant human immunodeficiency virus in vitro. Antimicrob. Agents Chemother. **51**:2143–2155.
2. **Antiretroviral Therapy Cohort Collaboration.** 2008. Life expectancy of individuals on combination antiretroviral therapy in high-income countries: a collaborative analysis of 14 cohort studies. Lancet **372**:293–299.
3. **Bhaskaran, K., O. Hamouda, M. Sannes, F. Boufassa, A. M. Johnson, P. C. Lambert, and K. Porter.** 2008. Changes in the risk of death after HIV seroconversion compared with mortality in the general population. JAMA **300**:51–59.
4. **Cho, A. E., V. Guallar, B. J. Berne, and R. Friesner.** 2005. Importance of accurate charges in molecular docking: quantum mechanical/molecular mechanical (QM/MM) approach. J. Comput. Chem. **26**:915–931.
5. **Clotet, B., N. Bellos, J. M. Molina, D. Cooper, J. C. Goffard, A. Lazzarin, A. Wohrmann, C. Katlama, T. Wilkin, R. Haubrich, C. Cohen, C. Farthing, D. Jayaweera, M. Markowitz, P. Ruane, S. Spinosa-Guzman, and E. Lefebvre.** 2007. Efficacy and safety of darunavir-ritonavir at week 48 in treatment-experienced patients with HIV-1 infection in POWER 1 and 2: a pooled subgroup analysis of data from two randomised trials. Lancet **369**:1169–1178.
6. **Condra, J. H., W. A. Schleif, O. M. Blahy, L. J. Gabryelski, D. J. Graham, J. C. Quintero, A. Rhodes, H. L. Robbins, E. Roth, M. Shivaprakash, et al.** 1995. In vivo emergence of HIV-1 variants resistant to multiple protease inhibitors. Nature **374**:569–571.
7. **De Clercq, E.** 2002. Strategies in the design of antiviral drugs. Nat. Rev. Drug Discov. **1**:13–25.
8. **de Mendoza, C., and V. Soriano.** 2004. Resistance to HIV protease inhibitors: mechanisms and clinical consequences. Curr. Drug Metab. **5**:321–328.
9. **De Meyer, S., H. Azijn, D. Surleraux, D. Jochmans, A. Tahri, R. Pauwels, P. Wigerinck, and M. P. de Bethune.** 2005. TMC114, a novel human immunodeficiency virus type 1 protease inhibitor active against protease inhibitor-resistant viruses, including a broad range of clinical isolates. Antimicrob. Agents Chemother. **49**:2314–2321.
10. **Erickson, J. W., and S. K. Burt.** 1996. Structural mechanisms of HIV drug resistance. Annu. Rev. Pharmacol. Toxicol. **36**:545–571.
11. **Ferrer, E., D. Podzamczer, M. Arnedo, E. Fumero, P. McKenna, A. Rinehart, J. L. Perez, M. J. Barbera, T. Pumarola, J. M. Gatell, and F. Gudiol.** 2003. Genotype and phenotype at baseline and at failure in human immunodeficiency virus-infected antiretroviral-naive patients in a randomized trial comparing zidovudine and lamivudine plus nelfinavir or nevirapine. J. Infect. Dis. **187**:687–690.
12. **Friesner, R. A., J. L. Banks, R. B. Murphy, T. A. Halgren, J. J. Klicic, D. T. Mainz, M. P. Repasky, E. H. Knoll, M. Shelley, J. K. Perry, D. E. Shaw, P. Francis, and P. S. Shenkin.** 2004. Glide: a new approach for rapid, accurate docking and scoring. 1. Method and assessment of docking accuracy. J. Med. Chem. **47**:1739–1749.
13. **Friesner, R. A., R. B. Murphy, M. P. Repasky, L. L. Frye, J. R. Greenwood, T. A. Halgren, P. C. Sanschagrin, and D. T. Mainz.** 2006. Extra precision glide: docking and scoring incorporating a model of hydrophobic enclosure for protein-ligand complexes. J. Med. Chem. **49**:6177–6196.
14. **Gatanaga, H., Y. Suzuki, H. Tsang, K. Yoshimura, M. F. Kavlick, K. Nagashima, R. J. Gorelick, S. Mardy, C. Tang, M. F. Summers, and H. Mitsuya.** 2002. Amino acid substitutions in Gag protein at non-cleavage sites are indispensable for the development of a high multitude of HIV-1 resistance against protease inhibitors. J. Biol. Chem. **277**:5952–5961.
15. **Ghosh, A. K., B. D. Chapsal, I. T. Weber, and H. Mitsuya.** 2008. Design of HIV protease inhibitors targeting protein backbone: an effective strategy for combating drug resistance. Acc. Chem. Res. **41**:78–86.
16. **Ghosh, A. K., P. R. Sridhar, S. Leshchenko, A. K. Hussain, J. Li, A. Y. Kovalevsky, D. E. Walters, J. E. Wedekind, V. Grum-Tokars, D. Das, Y. Koh, K. Maeda, H. Gatanaga, I. T. Weber, and H. Mitsuya.** 2006. Structure-based design of novel HIV-1 protease inhibitors to combat drug resistance. J. Med. Chem. **49**:5252–5261.
17. **Gong, Y. F., B. S. Robinson, R. E. Rose, C. Deminie, T. P. Spicer, D. Stock, R. J. Colonno, and P. F. Lin.** 2000. In vitro resistance profile of the human immunodeficiency virus type 1 protease inhibitor BMS-232632. Antimicrob. Agents Chemother. **44**:2319–2326.
18. **Gupta, R., A. Hill, A. W. Sawyer, and D. Pillay.** 2008. Emergence of drug resistance in HIV type 1-infected patients after receipt of first-line highly active antiretroviral therapy: a systematic review of clinical trials. Clin. Infect. Dis. **47**:712–722.
19. **Hertogs, K., S. Bloor, S. D. Kemp, C. Van den Eynde, T. M. Alcorn, R. Pauwels, M. Van Houtte, S. Staszewski, V. Miller, and B. A. Larder.** 2000. Phenotypic and genotypic analysis of clinical HIV-1 isolates reveals extensive protease inhibitor cross-resistance: a survey of over 6000 samples. AIDS **14**:1203–1210.
20. **Hicks, C. B., P. Cahn, D. A. Cooper, S. L. Walmsley, C. Katlama, B. Clotet, A. Lazzarin, M. A. Johnson, D. Neubacher, D. Mayers, and H. Valdez.** 2006. Durable efficacy of tipranavir-ritonavir in combination with an optimised background regimen of antiretroviral drugs for treatment-experienced HIV-1-infected patients at 48 weeks in the Randomized Evaluation of Strategic Intervention in multi-drug reSistant patients with Tipranavir (RESIST) studies: an analysis of combined data from two randomised open-label trials. Lancet **368**:466–475.
21. **Jacobsen, H., K. Yasargil, D. L. Winslow, J. C. Craig, A. Krohn, I. B. Duncan, and J. Mous.** 1995. Characterization of human immunodeficiency virus type 1 mutants with decreased sensitivity to proteinase inhibitor Ro 31–8959. Virology **206**:527–534.
22. **Kantor, R., W. J. Fessel, A. R. Zolopa, D. Israelski, N. Shulman, J. G.**

Montoya, M. Harbour, J. M. Schapiro, and R. W. Shafer. 2002. Evolution of primary protease inhibitor resistance mutations during protease inhibitor salvage therapy. Antimicrob. Agents Chemother. 46:1086–1092.
23. Kaplan, A. H., S. F. Michael, R. S. Wehbie, M. F. Knigge, D. A. Paul, L. Everitt, D. J. Kempf, D. W. Norbeck, J. W. Erickson, and R. Swanstrom. 1994. Selection of multiple human immunodeficiency virus type 1 variants that encode viral proteases with decreased sensitivity to an inhibitor of the viral protease. Proc. Natl. Acad. Sci. USA 91:5597–5601.
24. Kemper, C. A., M. D. Witt, P. H. Keiser, M. P. Dube, D. N. Forthal, M. Leibowitz, D. S. Smith, A. Rigby, N. S. Hellmann, Y. S. Lie, J. Leedom, D. Richman, J. A. McCutchan, and R. Haubrich. 2001. Sequencing of protease inhibitor therapy: insights from an analysis of HIV phenotypic resistance in patients failing protease inhibitors. AIDS 15:609–615.
25. Koh, Y., S. Matsumi, D. Das, M. Amano, D. A. Davis, J. Li, S. Leschenko, A. Baldridge, T. Shioda, R. Yarchoan, A. K. Ghosh, and H. Mitsuya. 2007. Potent inhibition of HIV-1 replication by novel non-peptidyl small molecule inhibitors of protease dimerization. J. Biol. Chem. 282:28709–28720.
26. Koh, Y., H. Nakata, K. Maeda, H. Ogata, G. Bilcer, T. Devasamudram, J. F. Kincaid, P. Boross, Y. F. Wang, Y. Tie, P. Volarath, L. Gaddis, R. W. Harrison, I. T. Weber, A. K. Ghosh, and H. Mitsuya. 2003. Novel bis-tetrahydrofuranylurethane-containing nonpeptidic protease inhibitor (PI) UIC-94017 (TMC114) with potent activity against multi-PI-resistant human immunodeficiency virus in vitro. Antimicrob. Agents Chemother. 47:3123–3129.
27. Li, F., R. Goila-Gaur, K. Salzwedel, N. R. Kilgore, M. Reddick, C. Matallana, A. Castillo, D. Zoumplis, D. E. Martin, J. M. Orenstein, G. P. Allaway, E. O. Freed, and C. T. Wild. 2003. PA-457: a potent HIV inhibitor that disrupts core condensation by targeting a late step in Gag processing. Proc. Natl. Acad. Sci. USA 100:13555–13560.
28. Little, S. J., S. Holte, J. P. Routy, E. S. Daar, M. Markowitz, A. C. Collier, R. A. Koup, J. W. Mellors, E. Connick, B. Conway, M. Kilby, L. Wang, J. M. Whitcomb, N. S. Hellmann, and D. D. Richman. 2002. Antiretroviral-drug resistance among patients recently infected with HIV. N. Engl. J. Med. 347:385–394.
29. Maeda, K., H. Nakata, Y. Koh, T. Miyakawa, H. Ogata, Y. Takaoka, S. Shibayama, K. Sagawa, D. Fukushima, J. Moravek, Y. Koyanagi, and H. Mitsuya. 2004. Spirodiketopiperazine-based CCR5 inhibitor which preserves CC-chemokine/CCR5 interactions and exerts potent activity against R5 human immunodeficiency virus type 1 in vitro. J. Virol. 78:8654–8662.
30. Maeda, K., K. Yoshimura, S. Shibayama, H. Habashita, H. Tada, K. Sagawa, T. Miyakawa, M. Aoki, D. Fukushima, and H. Mitsuya. 2001. Novel low molecular weight spirodiketopiperazine derivatives potently inhibit R5 HIV-1 infection through their antagonistic effects on CCR5. J. Biol. Chem. 276:35194–35200.
31. Maguire, M., D. Shortino, A. Klein, W. Harris, V. Manohitharajah, M. Tisdale, R. Elston, J. Yeo, S. Randall, F. Xu, H. Parker, J. May, and W. Snowden. 2002. Emergence of resistance to protease inhibitor amprenavir in human immunodeficiency virus type 1-infected patients: selection of four alternative viral protease genotypes and influence of viral susceptibility to coadministered reverse transcriptase nucleoside inhibitors. Antimicrob. Agents Chemother. 46:731–738.
32. Mammano, F., V. Trouplin, V. Zennou, and F. Clavel. 2000. Retracing the evolutionary pathways of human immunodeficiency virus type 1 resistance to protease inhibitors: virus fitness in the absence and in the presence of drug. J. Virol. 74:8524–8531.
33. McCallister, S., V. Kohlbrenner, K. Squires, A. Lazzarin, P. Kumar, E. DeJesus, J. Nadler, J. Gallant, S. Walmsley, P. Yeni, J. Leith, C. Dohnanyi, D. Hall, J. Sabo, T. MacGregor, W. Verbiest, P. McKenna, and D. Mayers. 2003. Characterization of the impact of genotype, phenotype, and inhibitory quotient on antiviral activity of tipranavir in highly treatment-experienced patients. Antivir. Ther. 8:S15.
34. Melamed, D., M. Mark-Danieli, M. Kenan-Eichler, O. Kraus, A. Custiel, N. Laham, T. Pupko, F. Glaser, N. Ben-Tal, and E. Bacharach. 2004. The conserved carboxy terminus of the capsid domain of human immunodeficiency virus type 1 Gag protein is important for virion assembly and release. J. Virol. 78:9675–9688.
35. Mitsuya, H., and J. Erickson. 1999. Discovery and development of antiretroviral therapeutics for HIV infection, p. 751–780. *In* T. C. Merigan, J. G. Bartlet, and D. Bolognesi (ed.), Textbook of AIDS medicine. The Williams & Wilkins Co., Baltimore, MD.
36. Mitsuya, H., K. Maeda, D. Das, and A. K. Ghosh. 2008. Development of protease inhibitors and the fight with drug-resistant HIV-1 variants. Adv. Pharmacol. 56:169–197.
37. Molla, A., M. Korneyeva, Q. Gao, S. Vasavanonda, P. J. Schipper, H. M. Mo, M. Markowitz, T. Chernyavskiy, P. Niu, N. Lyons, A. Hsu, G. R. Granneman, D. D. Ho, C. A. Boucher, J. M. Leonard, D. W. Norbeck, and D. J. Kempf. 1996. Ordered accumulation of mutations in HIV protease confers resistance to ritonavir. Nat. Med. 2:760–766.
38. Murphy, E. L., A. C. Collier, L. A. Kalish, S. F. Assmann, M. F. Para, T. P. Flanigan, P. N. Kumar, L. Mintz, F. R. Wallach, and G. J. Nemo. 2001. Highly active antiretroviral therapy decreases mortality and morbidity in patients with advanced HIV disease. Ann. Intern. Med. 135:17–26.
39. Murphy, R. L. 2000. New antiretroviral drugs in development. AIDS 14(Suppl. 3):S227–S234.
40. Partaledis, J. A., K. Yamaguchi, M. Tisdale, E. E. Blair, C. Falcione, B. Maschera, R. E. Myers, S. Pazhanisamy, O. Futer, A. B. Cullinan, C. M. Stuver, R. A. Byrn, and D. J. Livingston. 1995. In vitro selection and characterization of human immunodeficiency virus type 1 (HIV-1) isolates with reduced sensitivity to hydroxyethylamino sulfonamide inhibitors of HIV-1 aspartyl protease. J. Virol. 69:5228–5235.
41. Patick, A. K., M. Duran, Y. Cao, D. Shugarts, M. R. Keller, E. Mazabel, M. Knowles, S. Chapman, D. R. Kuritzkes, and M. Markowitz. 1998. Genotypic and phenotypic characterization of human immunodeficiency virus type 1 variants isolated from patients treated with the protease inhibitor nelfinavir. Antimicrob. Agents Chemother. 42:2637–2644.
42. Prado, J. G., T. Wrin, J. Beauchaine, L. Ruiz, C. J. Petropoulos, S. D. Frost, B. Clotet, R. T. D'Aquila, and J. Martinez-Picado. 2002. Amprenavir-resistant HIV-1 exhibits lopinavir cross-resistance and reduced replication capacity. AIDS 16:1009–1017.
43. Rodriguez-Barrios, F., and F. Gago. 2004. HIV protease inhibition: limited recent progress and advances in understanding current pitfalls. Curr. Top. Med. Chem. 4:991–1007.
44. Salzwedel, K., R. Goila-Gaur, C. Adamson, F. Li, A. Castillo, N. Kilgore, M. Reddick, C. Matallana, D. Zoumplis, D. Martin, G. Allaway, E. Freed, and C. Wild. 2004. Selection for and characterization of HIV-1 isolates resistant to the maturation inhibitor PA-457. Antivir. Ther. 9:S8.
45. Shirasaka, T., M. F. Kavlick, T. Ueno, W. Y. Gao, E. Kojima, M. L. Alcaide, S. Chokekijchai, B. M. Roy, E. Arnold, R. Yarchoan, et al. 1995. Emergence of human immunodeficiency virus type 1 variants with resistance to multiple dideoxynucleosides in patients receiving therapy with dideoxynucleosides. Proc. Natl. Acad. Sci. USA 92:2398–23402.
46. Walensky, R. P., A. D. Paltiel, E. Losina, L. M. Mercincavage, B. R. Schackman, P. E. Sax, M. C. Weinstein, and K. A. Freedberg. 2006. The survival benefits of AIDS treatment in the United States. J. Infect. Dis. 194:11–19.
47. Yoshimura, K., R. Kato, M. F. Kavlick, A. Nguyen, V. Maroun, K. Maeda, K. A. Hussain, A. K. Ghosh, S. V. Gulnik, J. W. Erickson, and H. Mitsuya. 2002. A potent human immunodeficiency virus type 1 protease inhibitor, UIC-94003 (TMC-126), and selection of a novel (A28S) mutation in the protease active site. J. Virol. 76:1349–1358.
48. Yoshimura, K., R. Kato, K. Yusa, M. F. Kavlick, V. Maroun, A. Nguyen, T. Mimoto, T. Ueno, M. Shintani, J. Falloon, H. Masur, H. Hayashi, J. Erickson, and H. Mitsuya. 1999. JE-2147: a dipeptide protease inhibitor (PI) that potently inhibits multi-PI-resistant HIV-1. Proc. Natl. Acad. Sci. USA 96:8675–8680.
49. Zhou, J., X. Yuan, D. Dismuke, B. M. Forshey, C. Lundquist, K. H. Lee, C. Aiken, and C. H. Chen. 2004. Small-molecule inhibition of human immunodeficiency virus type 1 replication by specific targeting of the final step of virion maturation. J. Virol. 78:922–929.